Soil Dynamics and Earthquake Engineering 173 (2023) 108140

Contents lists available at ScienceDirect

Soil Dynamics and Earthquake Engineering

journal homepage: www.elsevier.com/locate/soildyn

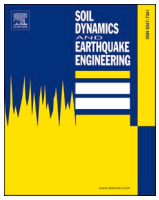

Study on the seismic mitigation effects of inerter isolated storage tanks

Chao Luo [a], Haoran Mu [b], Hao Wang [a,*], Xiaoxia Guo [b], Donglin Liu [b], Huaiping Feng [a]

[a] State Key Laboratory of Mechanical Behavior and System Safety of Traffic Engineering Structures, Shijiazhuang Tiedao University, Shijiazhuang, 050043, China
[b] School of Civil Engineering, Shijiazhuang Tiedao University, Shijiazhuang, 050043, China

ARTICLE INFO

Keywords:
Series viscous mass damper
Storage tanks
Seismic isolation
Wave height control
Inerter system
Hybrid control method

ABSTRACT

Liquefied Natural Gas (LNG) storage tanks can ensure national energy sufficiency, but they are vulnerable to earthquakes. Although ordinary seismic isolation bearings can effectively reduce the base shear force and overturning moment, they tend to amplify the height of the sloshing wave. In this paper, a hybrid vibration control method for LNG storage tanks is proposed, paralleling the series viscous mass damper (SVMD) devices with Lead-core rubber bearings (LRB). The seismic mitigation effects of this parallel seismic isolation scheme were investigated. First, three-dimensional finite element models of fixed base, LRB isolated and SVMD isolated tanks were established, and nonlinear time history analyses were performed for the three types of tanks to compare the seismic responses. It was concluded that SVMD can effectively control the sloshing wave height. In addition, the effects of site types, storage liquid heights, and SVMD's performance parameters on the seismic mitigation effects were also studied. It was found that the softer the site soil, the higher the storage liquid height would make seismic isolation less efficient. The increase of SVMD's additional equivalent mass reduces the sloshing wave height, increases the shear-to-weight ratio, and has little influence on the base displacement. The increase of SVMD's additional equivalent damping reduces the sloshing wave height, base shear force, and base displacement of the tank. The final conclusion is that SVMD can effectively control the sloshing wave height and has a good seismic mitigation effect.

1. Introduction

Liquefied Natural Gas (LNG) is a liquid formed after liquefaction of natural gas under ultra-low temperature and atmospheric pressure, and its volume is only 1/600 of that in the gaseous state, which has the advantages of easy transportation, flexibility, safety and efficiency, etc. It has gradually become the most active form of natural gas supply. Large LNG storage tanks (generally 100,000–200,000 m^3) are important unit equipments in LNG receiving terminals and account for a high proportion of investment in LNG receiving stations or peak-shaving liquefaction plant. Therefore, countries around the world attach great importance to the design and construction of large LNG storage tanks. Once the tank damaged in an earthquake, large amounts of flammable and explosive liquids may leak out, causing serious economic losses and casualties, and may also lead to explosions, fires and other devastating secondary disasters. Therefore, the safety of large LNG storage tanks under seismic action is particularly important.

Since the 1990s, many scholars have introduced seismic isolation technology into the field of seismic design of storage tanks. At present, tank seismic isolation mainly includes elastomeric seismic isolation system, friction sliding seismic isolation system, rolling seismic isolation system and hybrid seismic isolation system. The earliest seismic isolation device applied to tank-like structures is the laminated rubber bearings, and scholars have carried out a series of theoretical, simulation, experimental and application studies for this type of seismic isolation system. For natural rubber seismic isolation bearings, Chalhoub et al. [1] confirmed the effectiveness of seismic isolation by shaking table tests and verified the reliability of elastoplastic bearings in reducing the seismic response of tanks. Malhotra [2]} proposed ring beam isolation with soft rubber mats arranged around the tank's perimeter. The results of the numerical analysis show that the base isolation can significantly reduce the overturning moment of the tank and the axial stress of the tank wall under seismic action. Lead-core rubber bearings (LRB) can provide a certain damping ratio, so many scholars have also conducted studies on LRB-isolated storage tanks. Shrimali et al. [3] studied the seismic response of LRB isolated tanks under bidirectional seismic excitation and showed by theoretical analysis that lead core bearings can provide good seismic damping effect.

* Corresponding author.
E-mail address: wanghao@stdu.edu.cn (H. Wang).

https://doi.org/10.1016/j.soildyn.2023.108140
Received 12 January 2023; Received in revised form 12 July 2023; Accepted 21 July 2023
Available online 25 July 2023

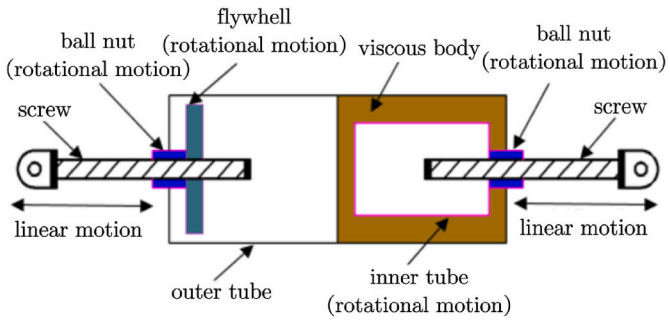

Fig. 1. Schematic diagram of the structure of SVMD.

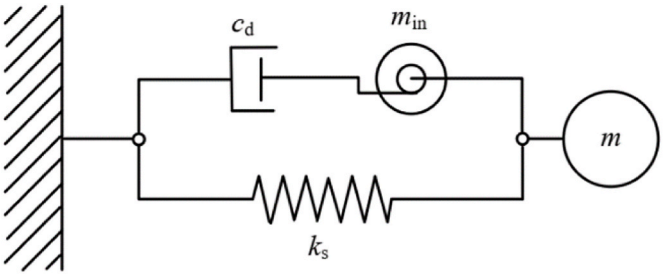

Fig. 2. Simplified analytical model of SVMD.

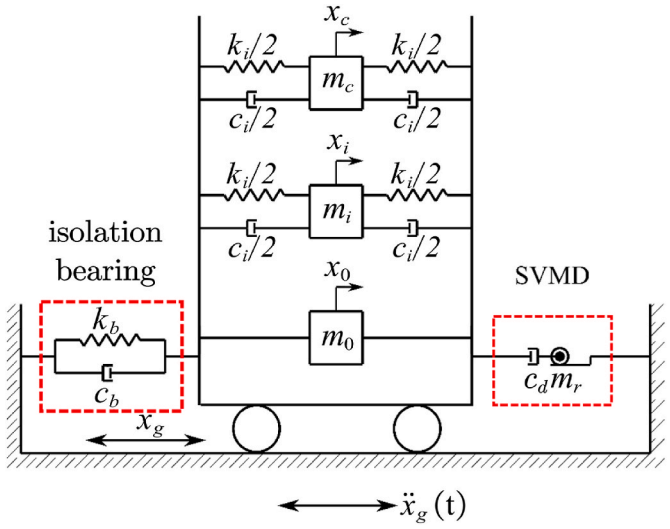

Fig. 3. Simplified mechanical model of the SVMD isolated storage tank.

Table 1
LNG storage tank's material properties.

Materials	Concrete	9% Ni steel (Minimum yield strength 490 MPa)	Liquefied Natural Gas
Density (kg/m^3)	2500	7850	450
Elasticity modulus (MPa)	3.35 × 10^4	2 × 10^5	2.56 × 10^2 (bulk modulus)
Poisson's ratio	0.2	0.3	

Curadelli [4] assumed that ground motion is a smooth stochastic process. An equivalent linearized stochastic seismic response analysis was carried out for the seismically isolated storage tank with LRB, and the effects of isolation period, yield force, viscous damping ratio and soil properties on the seismic isolation effect were investigated. Christovasilis [5] established a three-dimensional finite element model of the inner tank of the LNG storage tank to verify the seismic isolation effect of LRB and the accuracy of the bearing using a bilinear mechanical model. For different storage levels, the fundamental period of the tank structure is different. The friction sliding seismic isolation system can be effective in a wide range of frequencies, and the maximum acceleration transmitted to the structure can be controlled by the friction coefficient between the sliding surfaces. This advantage of the friction sliding seismic isolation system has led many scholars to conduct a lot of research on it, among which friction pendulum bearings and restoring force-friction bearings are the most widely used. In the study of friction pendulum bearings, in 2001, Wang et al. [6] proposed the application of friction pendulum isolation bearings to tank structures and verified the effectiveness of friction pendulum isolation for rigid cylindrical tanks through numerical simulations. Shrimali et al. [7] comparatively studied the seismic mitigation effects of various seismic isolation systems for storage tanks, such as laminated rubber bearings, LRBs, friction pendulum bearings and restoring force-friction bearings. The results showed that all the studied isolation systems can effectively attenuate the seismic acceleration transmitted to the tank structure, but the friction type isolation system is the most effective. Yu et al. [8] designed a seismic isolation system of friction pendulum bearing with U-shaped dampers. The shaking table test results showed that the isolation system can effectively reduce the dynamic water pressure and base displacement of the storage tank, and the system dissipated more seismic energy. Cheng et al. [9] proposed a simplified model for investigating a novel isolation system for rectangular concrete liquid storage tanks with sliding bases and displacement limiting devices. They found that the proposed system was able to prevent wall cracking and liquid spills. Zhang [10] et al. designed a seismic isolation system combining friction pendulum bearings and viscous dampers. The time history analysis showed that the system be effective in reducing the wave height and improving the seismic isolation performance of the tank, especially the isolation displacement. The rolling friction is smaller than the sliding friction generally, allowing a small seismic force to propagate to the upper structure, and the rolling isolation device is cheaper and easier to construct than the rubber bearings. So some scholars apply the rolling isolation device to the tank structure. Rawat [11] studied the developed oblate spheroid base isolation (OSBI) system. The system can dissipate the seismic energy input by rolling the installed ellipsoidal-shaped isolator on its horizontal axis and extend the fundamental period of the structure by oblateness. The authors used numerical integration techniques to perform mathematical derivations and motion control dynamics analysis of tanks fitted with nonlinear OSBI to reveal the underlying mechanisms behind their dynamic behavior.

Given the large displacement that occurs in the seismic isolation layer of large LNG storage tanks, researchers have recognized the need to incorporate energy dissipation damping devices to effectively dissipate seismic energy within the isolation layer. Currently, the main energy dissipation devices used in tank-type structures are viscous dampers and metallic yield dampers, etc. Malhotra et al. [12] proposed the method of anchoring the tank to the foundation with additional torsional-beam steel dampers at the perimeter to achieve energy dissipation damping. Angelis et al. [13] comparatively studied the dynamic response of tanks with fixed base, high damping rubber bearings and elasto-plastic dampers with slide isolators. Numerical analysis and shaking table tests have demonstrated that both isolation methods are effective in reducing the dynamic hydraulic pressure of the wall plate. Kharde et al. [14] proposed magneto-rheological dampers, derived the motion equations of intelligent systems, and solved them using the classical time-domain transformation matrix method. It was compared with a fixed base tank, a base isolation tank, and a tank with a passive magnetorheological damper. The results showed that smart base isolation can effectively reduce the seismic response of large LNG storage tanks, especially the displacement of the seismic isolation layer, without affecting other responses too much. Hao et al. [15] proposed a combined

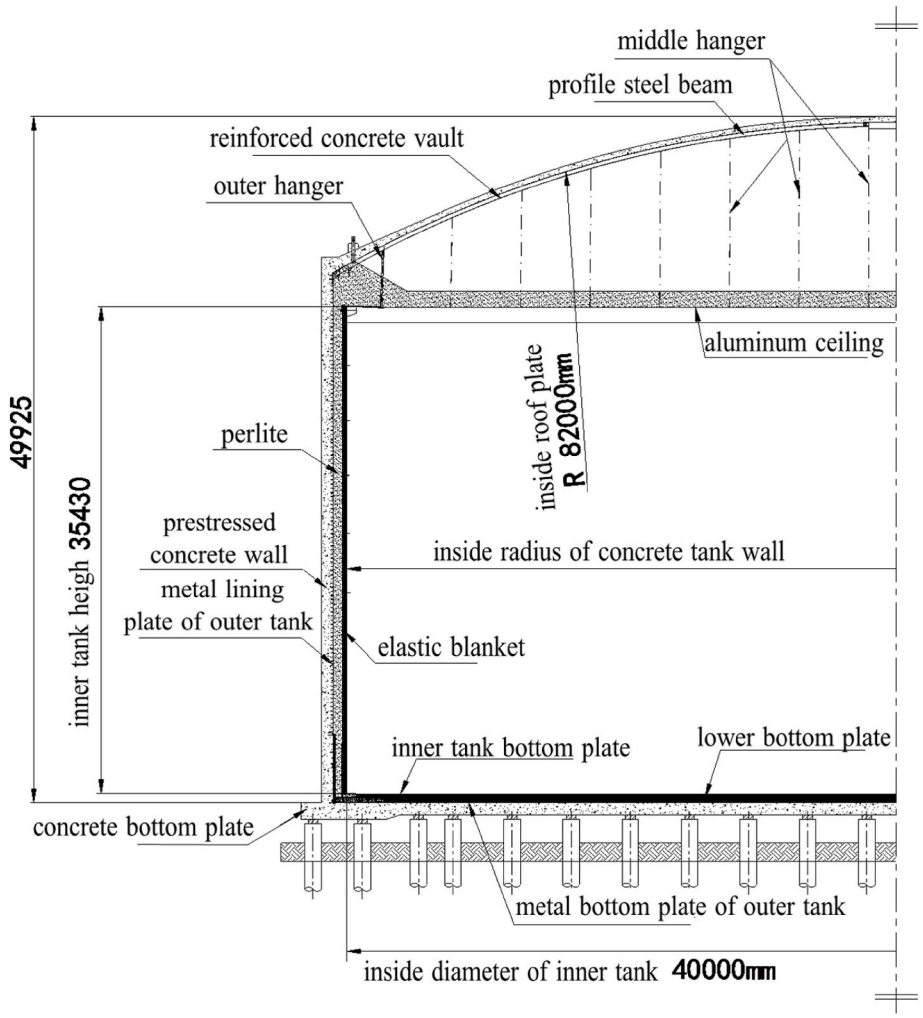

Fig. 4. Cross-sectional view of the tank.

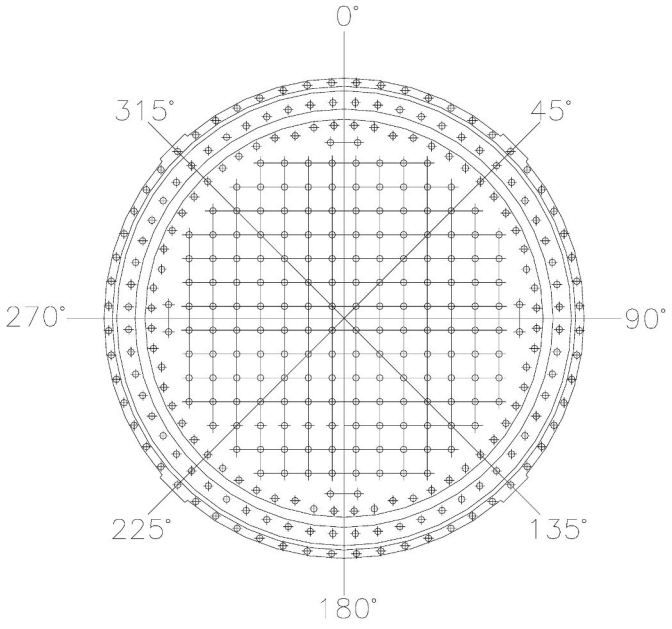

Fig. 5. Layout of seismic isolation bearings under the storage tank.

Table 2
Mechanical properties of lead-core rubber bearing.

Horizontal yielding force (kN)	Stiffness before yielding (kN/mm)	Stiffness after yielding (kN/mm)	Equivalent stiffness (kN/mm)
38160	5198	400	679 (horizontal displacement 120 mm)

seismic isolation method with additional viscous mass dampers in the seismically isolated storage tank, and verified through numerical simulation that the viscous mass dampers can effectively reduce the shaking response of the liquid in the storage tank. Zhang et al. [16] investigated the effects of different mechanical arrangements of inerter systems on seismic isolation tanks, and the designed tandem inerter system that could effectively reduce the seismic response of the storage tank under low frequency excitation, especially the isolation displacement. Jiang et al. [17] derived an optimal design equation for the inerter systems based on the target sloshing height mitigation ratio, which facilitates the preliminary design of inerter systems.

Summarize the above, scholars have conducted a lot of research on seismically isolated storage tank structures, and some of the research results have been successfully applied to the seismic design of storage tanks. The research results show that the base isolation technology can significantly reduce the base shear force, overturning moment and

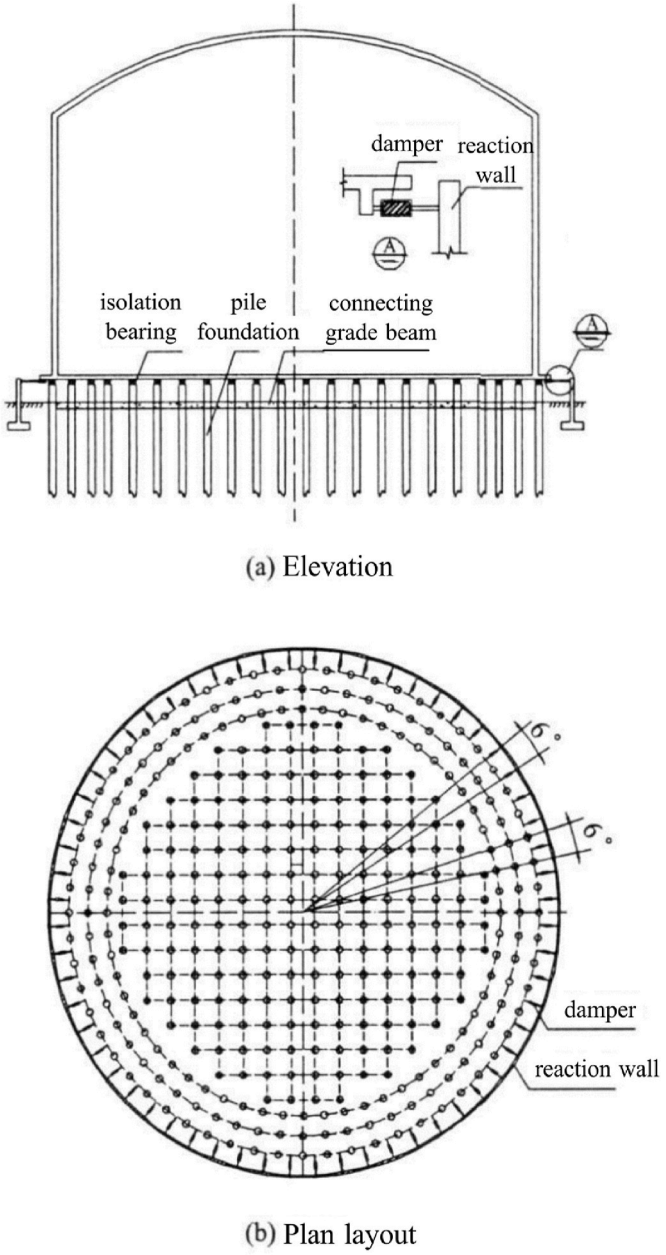

Fig. 6. Hybrid seismic isolated storage tank (a) Elevation, (b) Plan layout.

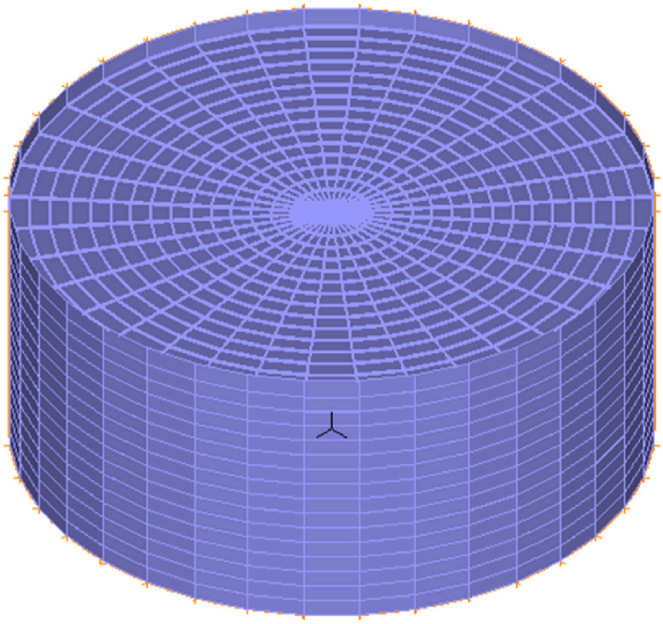

Fig. 7. Finite element model of the fixed base tank.

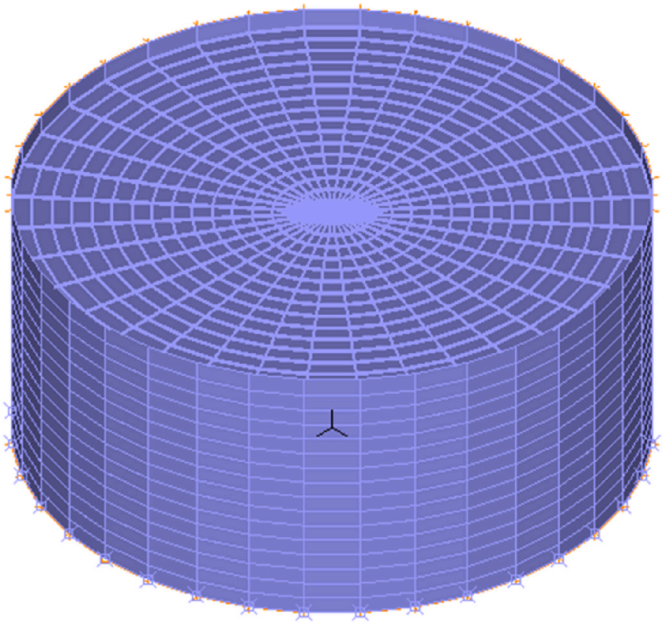

Fig. 8. Finite element model of the seismic isolated tank.

dynamic fluid pressure of the tank, which is an effective means to protect the tank from seismic damage. However, seismic isolation has not been found to have a significant limiting effect on the wave height of storage tanks, and there is even a wave height amplification effect, which is likely to cause overflow of stored liquid and buckling of the tank roof, etc. Therefore, there is an urgent need to explore a new seismic isolation technology, which can effectively control the vibration response of the storage fluid while reducing the overall seismic response of the tank. This project investigates a new LNG tank seismic isolation system combining seismic isolation bearings and series viscous mass damper (SVMD). The SVMD is a novel type of vibration control element composed of a series connection between a viscous damping unit and a mass unit. Compared with conventional vibration control elements, the advantages of SVMD are: 1) SVMD can adjust the inertia and stiffness characteristics of the structure, so that the frequency of the tank structure can be adjusted to avoid the resonance of the seismic isolation period with the liquid sloshing period and the resonance of the tank structure with horizontal seismic excitation. For large vertical acceleration, SVMD can be tuned to avoid the dominant frequency of vertical acceleration without changing the weight of the structure. 2) The vibration inside the SVMD system is not synchronized with the main structure. This asynchronous vibration can amplify the effective deformation of the energy dissipation device inside the system, thus providing efficient energy dissipation to further suppress the response. So with the addition of SVMD in the seismically isolated tank, the seismic input energy can be partially transferred to the additional mass-damping system, thus reducing the seismic energy input to the main structure of the tank and reducing the seismic response of the tank under the action of near-fault strong earthquakes. Compared with viscous dampers, SVMD can exert a greater energy dissipation effect and reduce the number of dampers arranged.

This paper firstly introduces the hybrid seismic mitigation control

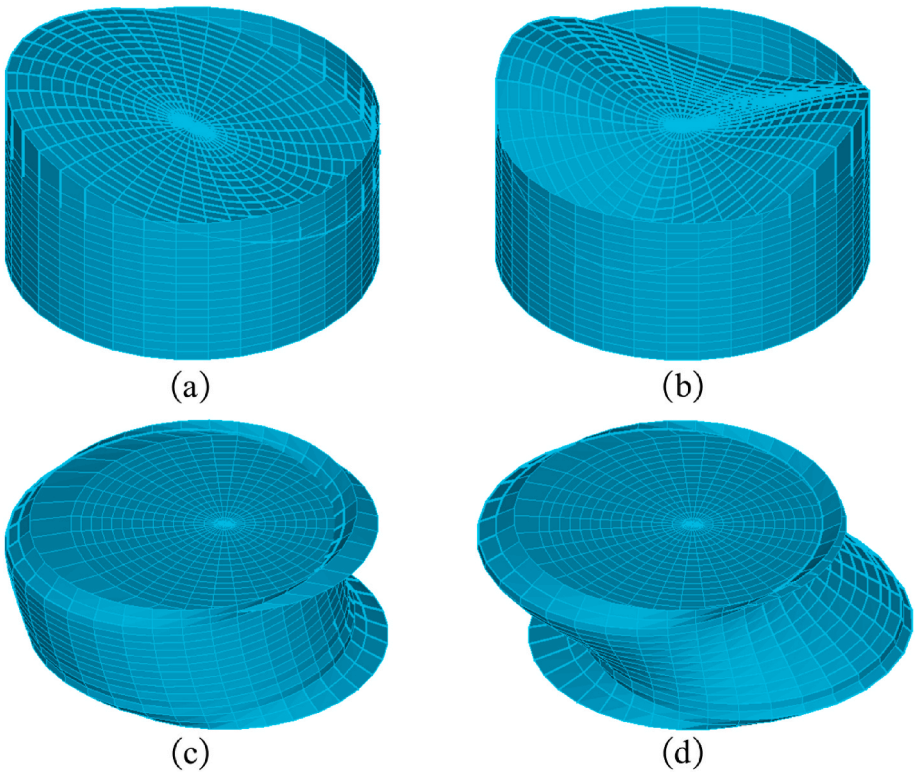

Fig. 9. (a) First liquid sloshing mode shape, (b) Second liquid sloshing mode shape, (c) First coupling mode shape, (d) Second coupling mode shape.

Table 3
Comparison of modal analysis results of the fixed base tank.

Modal	Theoretical solution		Three-dimensional finite element model	
	Frequency (Hz)	Period (s)	Frequency (Hz)	Period (s)
First coupling mode	1.7730	0.5640	1.689	0.5921
Second coupling mode	–	–	4.071	0.2456
First sloshing mode	0.1017	9.8387	0.1021	9.7943
Second sloshing mode	–	–	0.1371	7.2939

theory of LNG storage tanks, including the basic principle of vibration control of SVMD and the basic theory of hybrid seismic mitigation of storage tank with SVMD under horizontal seismic excitation. The seismic isolation design of a 160,000 m^3 LNG storage tank is introduced and the seismic responses of the isolated tank is analyzed through numerical simulation analysis. The seismic reduction effects of the seismic isolated tank with ordinary lead-core rubber bearings and with additional SVMD is compared. The effects of different site types on seismic mitigation effects are also studied. The difference of isolation effect when liquid storage height is different is studied, and the effect of the change of SVMD control parameters on seismic mitigation was explored.

2. Hybrid vibration control theory

2.1. Basic principles of SVMD control

Series Viscous Mass Damper (SVMD) is a new vibration control element developed from the principles of viscous damper, tuned mass damper and displacement efficiency mechanism. Its structure is shown in Fig. 1. SVMD mainly consists of two parts: one part mainly includes screw, ball nut and flywheel. The screw movement drives the flywheel for high-speed rotational motion, thus amplifying the mass effect of the flywheel. The other part mainly includes the screw, inner and outer barrel and viscous fluid, the screw movement drives the inner barrel for high-speed rotation, thus amplifying the damping effect of the viscous fluid. Because the displacements of the two elements are independent while the forces are common, the SVMD can be modeled by the series connection between the mass element and viscous damping element. Therefore, the simplified analytical model for an SVMD can be represented as shown in Fig. 2.

SVMD consists of a viscous damping unit and a mass unit connected in series, so the axial force of the damper can be expressed as

Table 5
Sloshing period coefficient.

D/H_w	0.6	1.0	1.5	2.0	2.5	3.0
Ks	1.047	1.047	1.054	1.074	1.105	1.141
D/H_w	3.5	4.0	4.5	5.0	5.5	6.0
Ks	1.184	1.230	1.277	1.324	1.371	1.418

Table 4
Coupling vibration period coefficients.

D/H_w	0.6	1.0	1.5	2.0	2.5	3.0
Kc	0.514×10^{-3}	0.44×10^{-3}	0.425×10^{-3}	0.435×10^{-3}	0.461×10^{-3}	0.502×10^{-3}
D/H_w	3.5	4.0	4.5	5.0	5.5	6.0
Kc	0.537×10^{-3}	0.58×10^{-3}	0.62×10^{-3}	0.681×10^{-3}	0.736×10^{-3}	0.791×10^{-3}

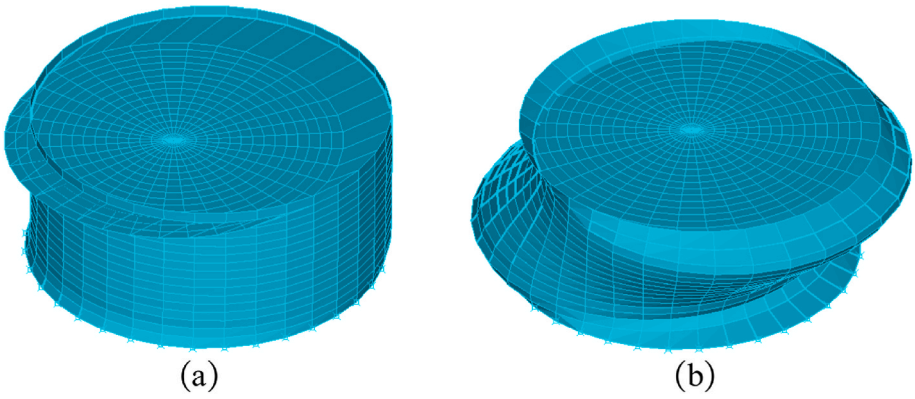

Fig. 10. (a) First and (b) Second coupling mode shapes of the seismic isolated tank with lead rubber bearings.

Table 6
Comparison of modal analysis results of the LRB isolated tank.

Modal	Theoretical solution		Three-dimensional finite element model	
	Frequency (Hz)	Period (s)	Frequency (Hz)	Period (s)
First coupling mode	0.4717	2.1199	0.477	2.0964
Second coupling mode	–	–	3.922	0.2549

Table 7
Ground motion records for seismic response analysis.

Year	Site	Magnitude	Epicentral Distance	Shear Wave Velocity
1989	Loma Prieta	6.93	45.42	126.4
2000	Tottori_Japan	6.61	16.6	138.76
2004	Niigata_Japan	6.63	25.14	128.12
2007	Chuetsu-oki_Japan	6.8	21.37	128.12
2008	Iwate Japan	6.9	74.75	135.4

$$p = c_d \dot{x}_c = m_r \ddot{x}_r$$

where, p is the axial out force of the damper; $\dot{x}_c$ is the axial velocity of the viscous unit of the damper; $\ddot{x}_r$ is the axial acceleration of the equivalent additional mass of the damper.

The equivalent mass m_r and the damping factor c_d can be expressed respectively as

$$m_r = S_i^2 \frac{1}{2}\left(r_o^2 + r_i^2\right) m_0$$

$$c_d = S_v^2 \frac{\upsilon A}{d_y}$$

where, S_i is the ratio of the circumferential acceleration of the steel tube inner surface to the axial linear acceleration; r_o is the outer radius of the additional mass; r_i is the inner radius of the additional mass; m_0 is the actual mass of the additional mass part of the damper; S_v is the ratio of the circumferential velocity of the inner surface of the tube to the axial linear velocity; υ is the kinematic viscosity of the viscous material; A is the lateral area of the rotating inner tube; d_y is the distance between the inner and outer tubes. The equivalent mass of the damper's mass unit can be scaled up relative to the actual mass at $S_i^2 \frac{1}{2}(r_o^2 + r_i^2)$. The scale value can reach several thousand times the actual mass.

2.2. Seismic mitigation theory of SVMD isolated tanks

This study proposes a hybrid seismic isolation system for LNG

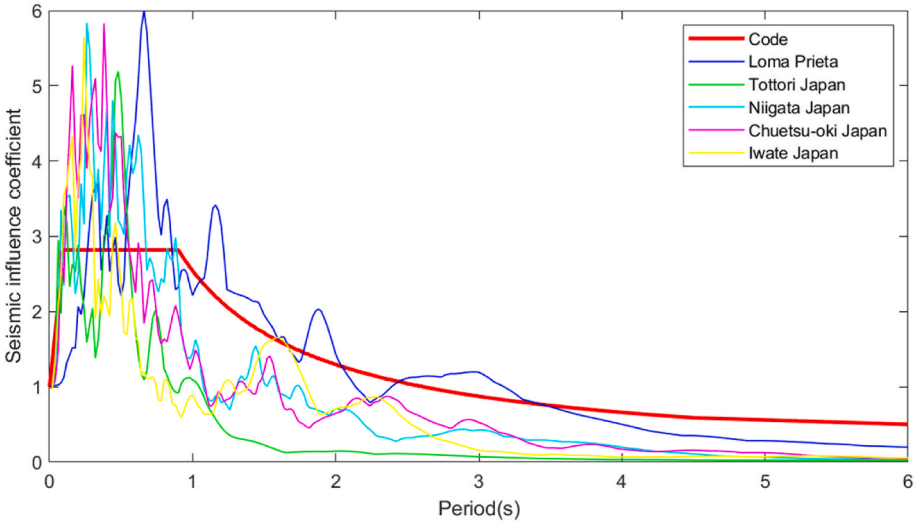

Fig. 11. Response spectrum of the ground motion records.

Table 8
Maximum sloshing wave height.

Work Conditions	Structure Type	Maximum Sloshing Wave Height (m)					
		Loma Prieta	Tottori	Niigata	Chuetsu-oki	Iwate	Average Value
OBE	ST0	0.677	0.293	0.946	0.833	1.320	0.8138
	ST1	0.716	0.343	1.049	0.941	1.367	0.8832
	ST2	0.613	0.259	0.803	0.652	1.256	0.7166
SSE	ST0	1.592	0.550	1.513	2.357	1.607	1.5238
	ST1	1.671	0.736	1.932	2.562	1.930	1.7802
	ST2	1.465	0.504	1.340	2.079	1.505	1.3786

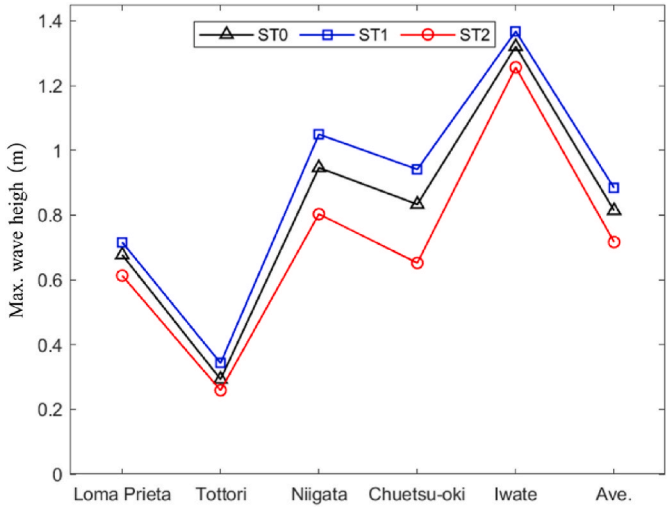

Fig. 12. Tank sloshing wave height (OBE).

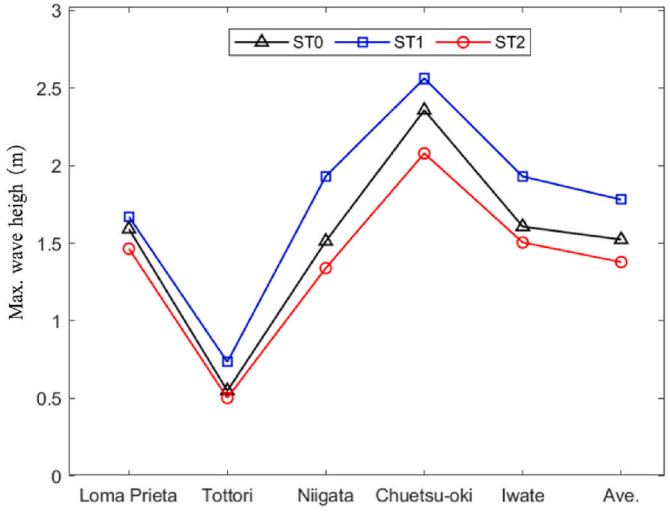

Fig. 13. Tank sloshing wave height (SSE).

storage tanks by combining seismic isolation bearings and SVMD. The main purpose is to control the sloshing wave height with the addition of SVMD in the seismically isolated tank. At the same time, the seismic input energy can be partially transferred to the additional mass-damping system. The vibration control schematic is shown in Fig. 3.

Assuming that the tank is excited by the ground motion $\ddot{x}_g(t)$, the motion equations of the SVMD isolated tank system are

$$m_c\ddot{x}_c + c_c(\dot{x}_c - \dot{x}_b) + k_c(x_c - x_b) = -m_c\ddot{x}_g$$
$$m_i\ddot{x}_i + c_i(\dot{x}_i - \dot{x}_b) + k_i(x_i - x_b) = -m_i\ddot{x}_g$$
$$m_b\ddot{x}_b + c_b\dot{x}_b + k_bx_b + p_d + m_c\ddot{x}_c + m_i\ddot{x}_i = -\widetilde{m}\ddot{x}_g$$
$$p_d = m_r\ddot{x}_b + c_d\dot{x}_b$$

where, x_c , x_i , x_b are the displacements of the convective component, the impulsive component and the tank base, respectively, p_d is the longitudinal damping force provided by SVMD, $\widetilde{m}$ is the total mass of the reservoir and the tank base, expressed as Eq. (5)

$$\widetilde{m} = m_c + m_i + m_b$$

By the Newmark algorithm, Eq. (4) can be easily solved to obtain the numerical solution of the seismic isolation tank, so as to obtain the seismic response of the isolation tank system.

For a seismic isolation tank with SVMD, the damping force provided by the SVMD is related to the base response, which is strongly influenced by the impulse component. Therefore, the equivalent mass and equivalent viscous damping of the SVMD can be adjusted according to the corresponding parameters of the impulse component

$$m_r = \mu m_i$$
$$c_d = \eta c_i$$

where, μ and η are the mass and damping adjustment factors of the SVMD, respectively.

3. Numerical model

3.1. Project overview

An examination of a storage tank project using hybrid isolation and control is given as an example. The LNG storage tank type is a full containment tank. The main parameters of the tank are as follows: networking volume is 160,000 m^3, design liquid density is 480 kg/m^3, design inlet rate is 12,100 m^3/h, design outlet rate is 1260 m^3/h, maximum design pressure is 290 mbarg, and design LNG temperature is $-170\ ^\circ C$. The tank wall parameters are as follows: the inner diameter of the inner tank is 80.0 m, height is 35.43 m; the inner tank is made of nickel steel, whose density is about 7.85×10^3 kg/m^3; the thickness of the inner tank is 24.9 mm at the bottom and 12 mm at the top. The insulation layer is made of an elastic blanket and perlite. The thickness of the elastic blanket is 300 mm and the density is 16.0 kg/m^3. The thickness of the perlite is about 700 mm and the density is about 65.0 kg/m^3. The inner diameter of the concrete outer tank wall is 82.0 m. The outer tank's height is 38.55 m and its thickness is 0.8 m. The concrete wall's density is about 2450 kg/m^3. The concrete bottom plate's diameter is 86.6 m and thick is 1.2 m. The concrete tank's top thickness is 0.4 m. The inner tank's height is 34.43 m, and the concrete's top height is 49.925 m. The normal operation maximum liquid level is 34.26 m. Materials of storage tank properties are shown in Table 1. The tank cross-sectional view is shown in Fig. 4. The tank's peak horizontal ground motion acceleration is 0.09g for OBE (Operational Basis Earthquake) condition and 0.37g for SSE (Safety Shutdown Earthquake) condition.

This study's main aim is to investigate the passive control effects of

Table 9
Maximum base displacement.

Work Conditions	Structure Type	Maximum Base Displacement (m)					
		Loma Prieta	Tottori	Niigata	Chuetsu-oki	Iwate	Average Value
OBE	ST0	0	0	0	0	0	0
	ST1	0.056	0.053	0.058	0.059	0.048	0.0548
	ST2	0.056	0.040	0.049	0.047	0.052	0.0488
SSE	ST0	0	0	0	0	0	0
	ST1	0.122	0.106	0.131	0.120	0.073	0.1104
	ST2	0.120	0.085	0.108	0.104	0.081	0.0996

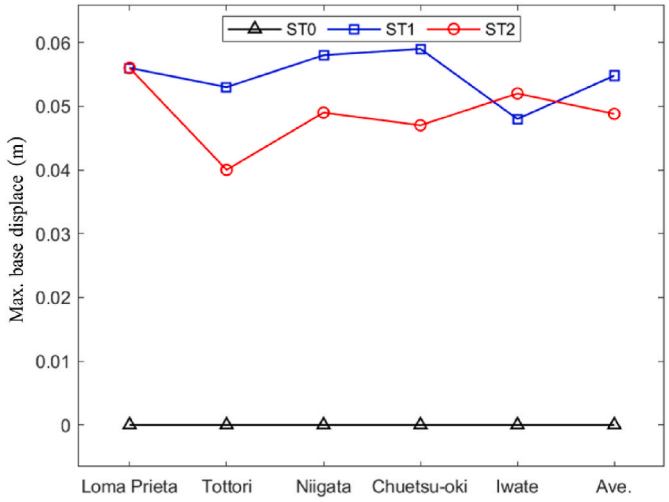

Fig. 14. Maximum base displacement of the storage tanks under different seismic waves.

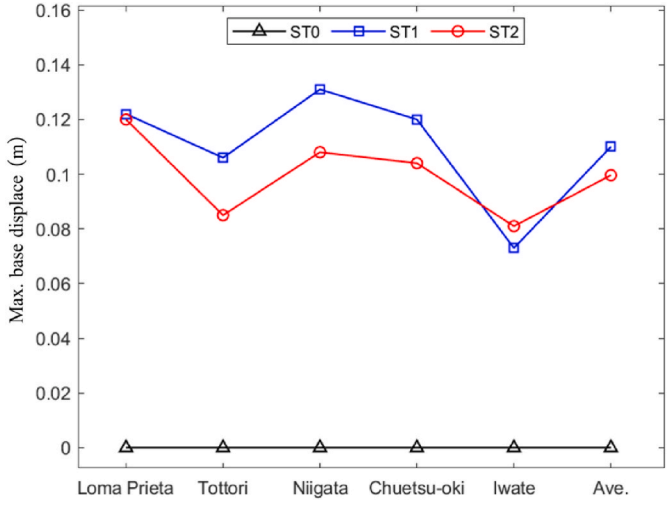

Fig. 15. Maximum base displacement of the storage tanks under different seismic waves.

the seismic isolation bearings in combination with SVMD. As a result, the isolation design of the storage tank was carried out and three groups of comparison conditions were set. The three tank designs are respectively fixed base tank (ST0) , seismic isolated tank with lead rubber bearings (ST1) , and seismic isolated tank with lead rubber bearings and SVMD (ST2). For the seismic isolated tank with lead rubber bearings (ST1), the tank is designed to place on 360 lead rubber bearings and each bearing's size is Φ700 × 253 mm. The seismic isolation bearings are installed at the top of the pile foundation, and the layout of seismic isolation bearings is shown in Fig. 5, and the mechanical properties of lead rubber bearings are shown in Table 2. For the seismic isolated tank with lead rubber bearings and SVMD (ST2), the hybrid seismic isolation system includes SVMD, reaction wall and seismic isolation bearings. According to Fig. 6, the reaction wall is connected to the SVMD, which is placed in a circle along the base of the tank, and the seismic isolation bearings are installed at the top of the pile foundation. The SVMD's additional damping [15] is set 0.8 times equivalent viscous damping of the pulse component *cb*, and the SVMD's additional mass is 0.6 times the pulse mass *mr*.

3.2. Finite element model

The inner tank wall and bottom plate of the storage tank adopt shell elements. The storage liquid is set as a non-spinning, non-viscous, non-heat transfer liquid, and the liquid level is designated as a free liquid. The vertical direction of the tank is divided into 16 units, and the vertical direction of the liquid is divided into 15 units. The structural model of the non-seismic storage tank is shown in Fig. 7. The Rayleigh damping of the inner tank is calculated based on the first two orders of coupled fundamental frequencies $f_1 = 1.689$Hz, $f_2 = 4.071$Hz and the 2% coupling vibration damping ratio ξ_1 of the liquid and elastic tank wall.

For the seismic isolated tank with lead rubber bearings (ST1), the bearings adopt spring elements to provide stiffness and damping to the seismic isolation structure. The damping ratio ξ of the isolation layer is 0.2. 360 lead-core rubber bearings are set in the model, the total stiffness of the bearing of the seismic isolation layer *kb* is 679 kN/mm, and the seismic isolation tank structure model is shown in Fig. 8.

For the seismic isolated tank with lead rubber bearings and SVMD (ST2), the SVMD adopt spring elements to provide damping and mass to the seismic isolation structure. The total damping *cb* of the seismic isolation layer can be calculated according to Eq. (7).

$$c_b = \xi m \frac{4\pi}{T_b}$$

where, *Tb* is seismic isolation period, *kb* is total stiffness of the seismic isolation layer, *cb* is total damping of the seismic isolation layer, *m* is total mass of the storage tank, ξ is viscous damping ratio.

3.3. Dynamic characteristics

Based on the modal analysis of the finite element model, the vibration patterns of the fixed base tank are shown in Fig. 9. The first two periods of the tank are shown in Table 3. According to the modal analysis, the following conclusions can be obtained: 1) The first sloshing mode of the fixed base tank is liquid sloshing mode shape, and the first coupling mode is beam type mode shape. 2) The representative value of the gravity load of the superstructure is 77380.4t. 3) The fundamental period of the fixed base tank is 0.1s < 0.5921s < 0.9s (Tg).

To verify the reliability of the finite element model, the modal frequencies calculated by the finite element modal are compared to theoretical solution. The basic period *Tc* of liquid-tank coupling vibration of storage tanks can be calculated approximately according to Eq. (8) [18].

Table 10
Maximum base shear/weight.

Work Conditions	Structure Type	Maximum Base Shear/Weight					
		Loma Prieta	Tottori	Niigata	Chuetsu-oki	Iwate	Average Value
OBE	ST0	0.2519	0.2123	0.1635	0.2281	0.2651	0.22418
	ST1	0.0471	0.0444	0.0488	0.0502	0.0409	0.04628
	ST2	0.0480	0.0365	0.0447	0.0431	0.0497	0.04440
SSE	ST0	0.5710	0.5433	0.4457	0.6422	0.6831	0.57706
	ST1	0.1069	0.0964	0.1156	0.1067	0.0770	0.10048
	ST2	0.1089	0.0927	0.0985	0.0924	0.0628	0.09106

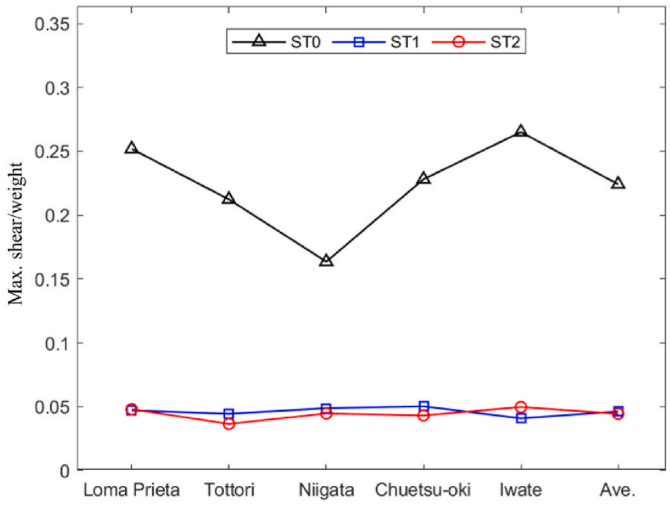

Fig. 16. Maximum base shear-to-weight ratio of liquid storage tanks under different seismic waves.

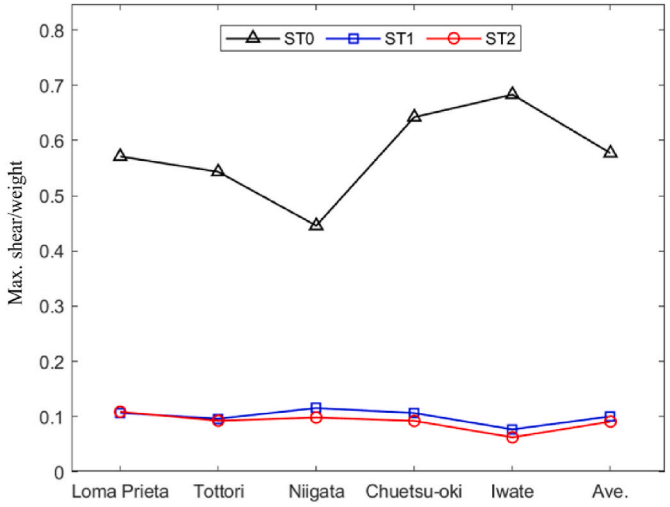

Fig. 17. Maximum base shear-to-weight ratio of liquid storage tanks under different seismic waves.

$$T_c = K_c H_w \sqrt{\frac{R}{\delta_{1/3}}}$$

where, *Tc* is the basic period of liquid-tank coupling vibration of storage tanks, *R* is the inner radius of the storage tank (m), $\delta_{1/3}$ is the effective thickness of the tank wall at 1/3 height from the bottom plate, *HW* is the design liquid depth of the tank (m), *KC* is the coupling vibration period coefficient, according to the value of *D/HW* in Table 4.

The liquid-tank vibration period *Tw* can be calculated according to Eq (9) [18].

$$T_w = K_s \sqrt{D}$$

where, *Tw* is the basic period of liquid storage sloshing (s), *KS* is the sloshing period coefficient, according to *D/Hw* in Table 5, and *D* is the inner diameter of the tank (m).

The comparison results between Eq. (8)–(9) and the finite element modal are shown in Table 3. It is shown that the error of the first coupling modal frequency of the structure does not exceed 5%, and the error of the first sloshing modal frequency does not exceed 1%, which proves the reliability of the finite element model.

Furthermore, the modal analysis was conducted on the seismic isolated tank with lead rubber bearings (ST1). The first and second coupling vibration mode of the seismic isolation structure is shown in Fig. 10. The first two periods are shown in Table 6.

The modal frequencies of the seismic isolated tank with lead rubber bearings (ST1) calculated by the finite element modal are compared to the theoretical solution. According to Eq. (8) [18], the coupled natural vibration period *Tb* of the isolated tank is 2.12s, and the natural vibration frequency is 0.4717Hz. The first coupling self-oscillation frequency of the isolated tank calculated by the finite element model is 0.477Hz. The frequency of the finite element model is consistent with the theoretical solution.

4. Nonlinear time history analysis

4.1. Ground motion selection

Five ground motion acceleration records are selected from the Pacific Earthquake Engineering Research Center (PEER) database for the seismic response analysis of the storage tank. The type of site soil is Class IV. The site soil cover depth is greater than 80 m and the equivalent shear wave velocity of the site soil is less than or equal to 150 m/s. The site soil is soft soil. The design seismic group is the third group. The site characteristic period of 0.9s is selected. The basic information of the ground motion records is shown in Table 7 and is consistent with the seismic design code response spectrum [19], as shown in Fig. 11.

4.2. Maximum sloshing wave height

The maximum wave height of the storage tank under different seismic ground motions is obtained from nonlinear time history analysis, as shown in Table 8, Fig. 12 and Fig. 13. In these figures, ST0, ST1 and ST2 indicate the fixed base tank, LRB isolated tank and SVMD isolated tank, respectively. From Table 8, Figs. 12 and 13, it can be seen that the wave heights of the LRB isolated tank are 8.53% and 16.82% larger than those of the fixed base tank under OBE and SSE conditions, indicating that the ordinary seismic isolation measures not only fail to reduce the wave height of the tank but also increase the wave height response. The wave height of the SVMD isolated tank is reduced to 88.06% and 90.47% of the fixed base tank on average under OBE and SSE conditions, respectively. It indicates that the wave height is effectively controlled by SVMD isolation.

Table 11
Comparison of the maximum effective stress on the tank wall.

Work Conditions	Structure Type	Maximum Effective Stress (MPa)					
		Loma Prieta	Tottori	Niigata	Chuetsu-oki	Iwate	Average Value
OBE	ST0	270	277	258	281	299	277
	ST1	207	210	214	213	205	209.8
	ST2	206	208	209	212	203	207.6
SSE	ST0	421	369	366	449	456	412.2
	ST1	240	237	248	245	221	238.2
	ST2	231	223	235	227	220	227.2

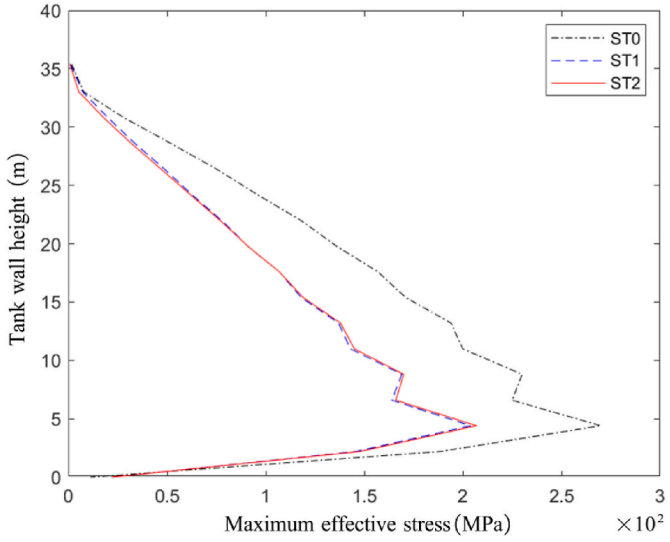

Fig. 18. Distribution of the maximum effective stress (OBE) under the Loma Prieta wave.

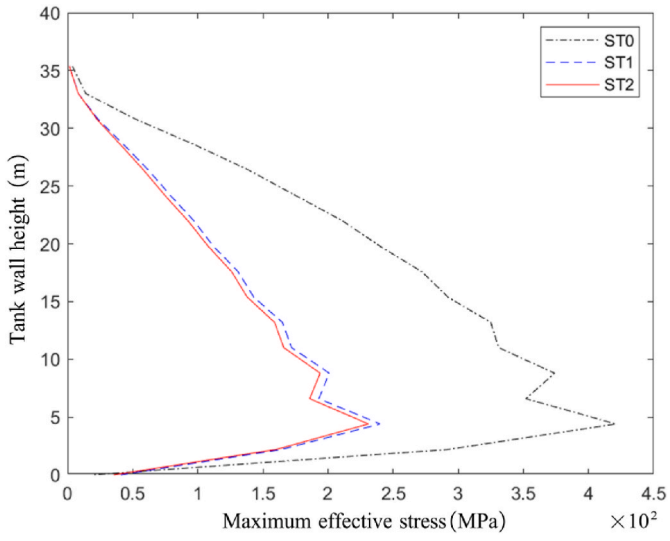

Fig. 19. Distribution of the maximum effective stress (SSE) under the Loma Prieta wave.

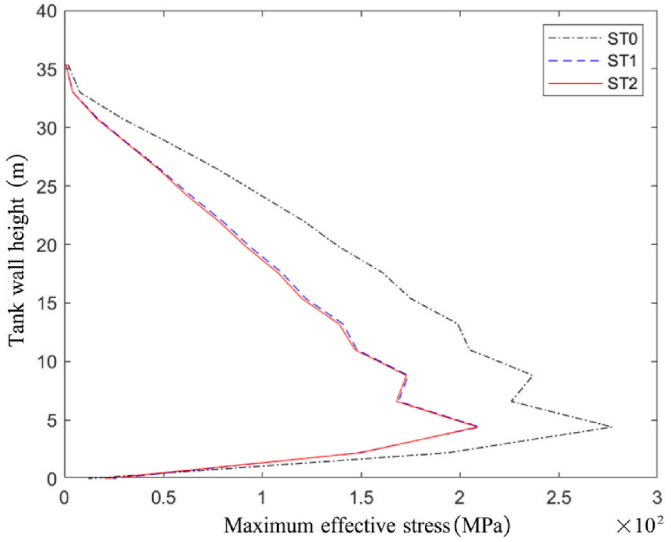

Fig. 20. Distribution of the maximum effective stress (OBE) under the Tottori wave.

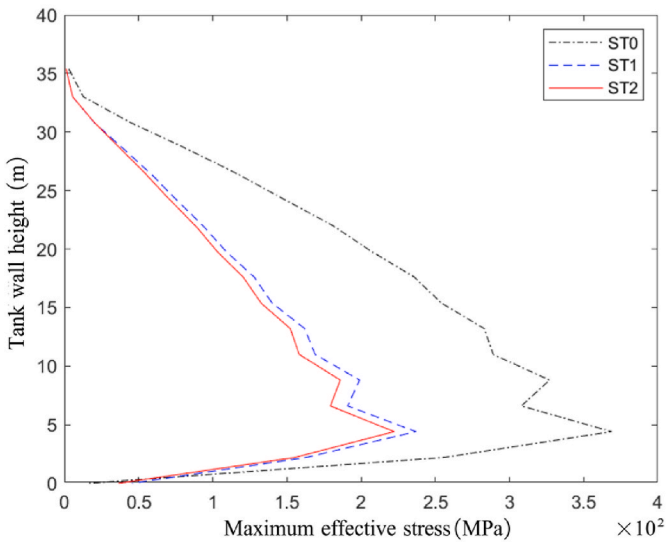

Fig. 21. Distribution of the maximum effective stress (SSE) under the Tottori wave.

4.3. Maximum base displacement

The maximum base displacements of the storage tank under different seismic ground motions are obtained from nonlinear time history analysis, as shown in Table 9, Fig. 14 and Fig. 15. It can be seen from Table 9, Figs. 14 and 15 that the maximum base displacements of the SVMD isolated tank under three out of five ground motions are significantly decreased compared with that of the LRB isolated tank under OBE condition. The average value of the maximum base displacement of the LRB isolated tank is 0.0548 m, and that of the SVMD isolated tank is 0.0488 m. The average value of the maximum base displacement of the SVMD isolated tank is 10.95% smaller than that of the LRB isolated tank.

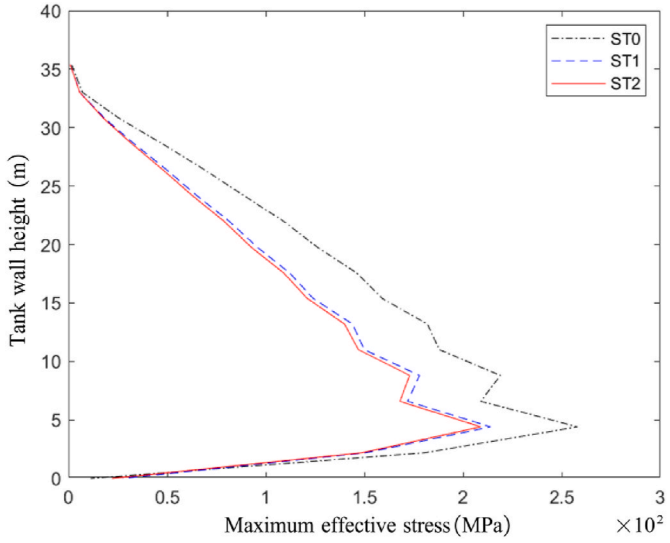

Fig. 22. Distribution of maximum effective stress (OBE) under the Niigata wave.

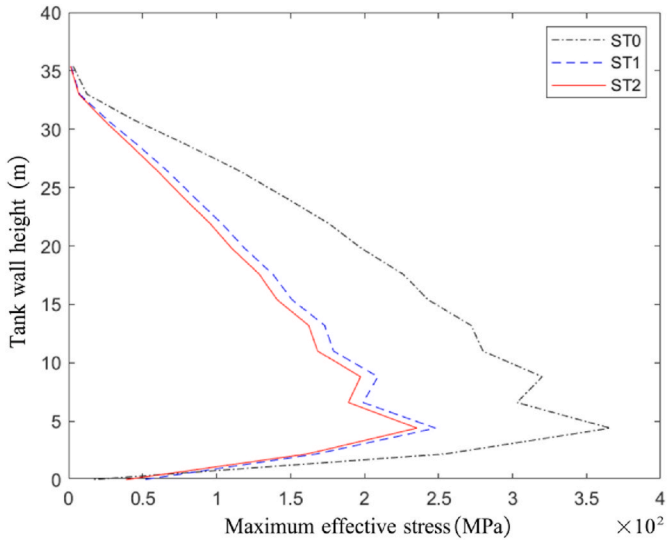

Fig. 23. Distribution of maximum effective stress (SSE) under the Niigata wave.

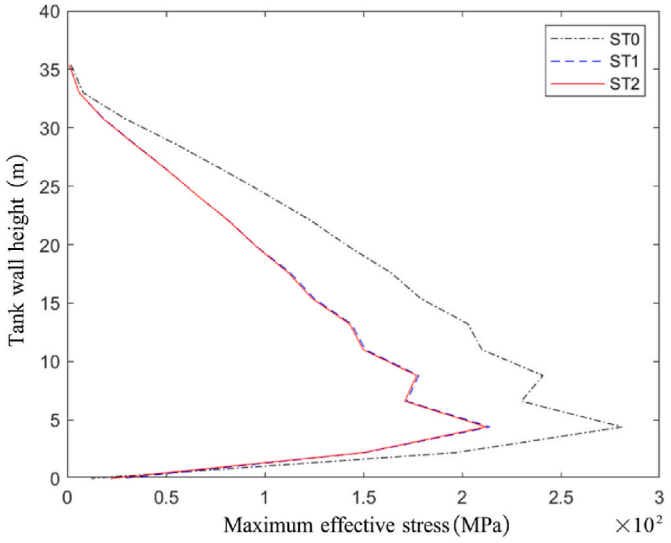

Fig. 24. Distribution of maximum effective stress (OBE) under the Chuetsu-oki wave.

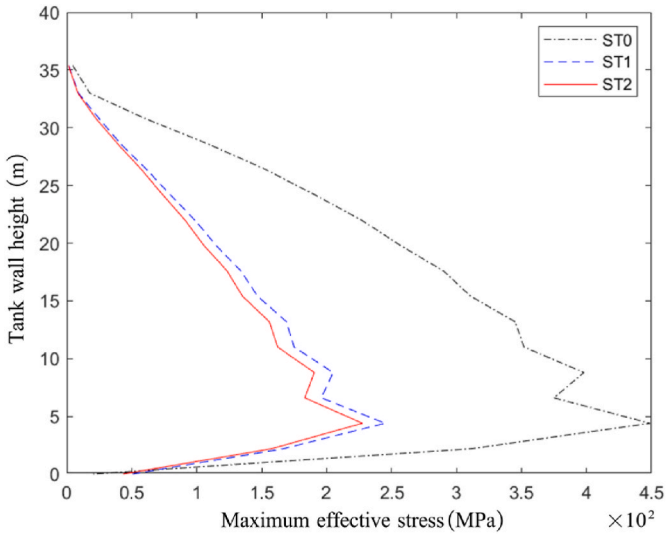

Fig. 25. Distribution of maximum effective stress (SSE) under the Chuetsu-oki wave.

Under SSE condition, the displacement of the isolation layer of the SVMD isolated tank under four out of five ground motions is significantly decreased compared with the LRB isolated tank. The average value of the maximum base displacements of the LRB isolated tank is 0.1104 m, and that of the SVMD isolated tank is 0.0996 m. The average value of the maximum base displacements of the SVMD isolated tank is reduced to 90.22% compared to that of the LRB isolated tank. It can be seen that the SVMD device can effectively reduce the displacement of the seismic isolation layer, and the control effect weakens with the increase of seismic intensity.

4.4. Maximum base shear

Table 10, Fig. 16 and Fig. 17 show the ratio of the maximum base shear to weight of the structure. It can be seen that the ratios of base-shear to weight of the isolated tank under five ground motions are significantly reduced compared with the fixed-base tank under OBE and SSE conditions. Under OBE condition, the average ratio of base-shear to weight of LRB isolated tank is reduced to 20.64% of fixed base tank, and that of SVMD isolated tank is reduced to 19.81% of fixed base tank. Under SSE condition, the average ratio of base-shear to weight of LRB isolated tank is reduced to 17.41% of fixed base tank, and that of SVMD isolated tank is reduced to 15.78% of fixed base tank.

Under OBE condition, the ratios of base-shear to weight of SVMD isolated tank are 101.91%, 82.21%, 91.60%, 85.86% and 121.52% of LRB isolated tank, respectively, with the average value reduced to 95.94% of LRB isolated tank. Under SSE condition, the ratios of base-shear to weight of SVMD isolated tank are 101.87%, 96.16%, 85.21%, 86.60% and 81.56% of LRB isolated tank, respectively, with the average value reduced to 90.63% of LRB isolated tank. It can be concluded that the seismic isolation measures can significantly reduce the base shear of the structure, and the use of SVMD can further reduce the structure's base shear and increase the structure's safety. And the base shear mitigation effects increase with the increase in seismic intensity.

4.5. Maximum effective stress

The maximum effective stresses on the tank wall are shown in

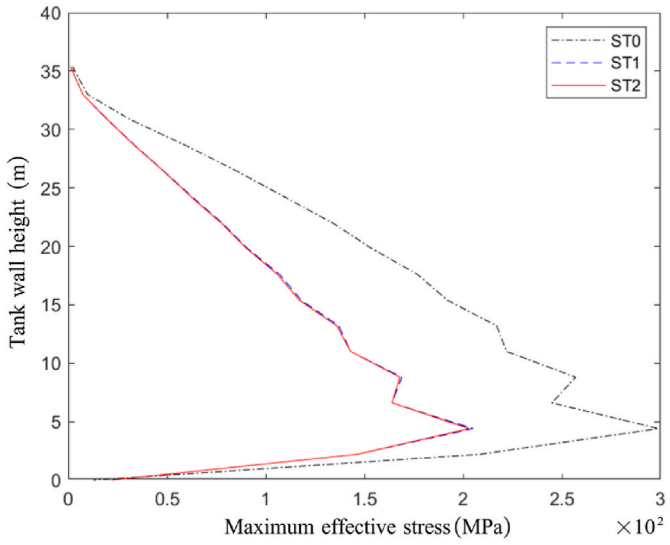

Fig. 26. Distribution of maximum effective stress (OBE) under the Iwate wave.

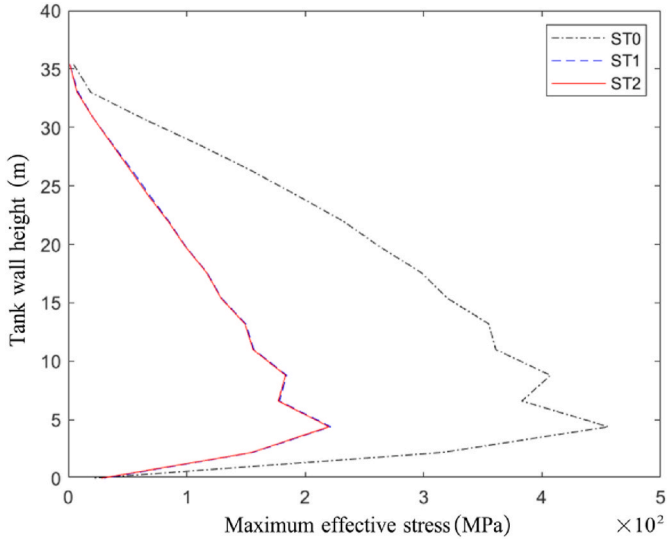

Fig. 27. Distribution of maximum effective stress (SSE) under the Iwate wave.

Table 11, the distributions of the maximum effective stress along the height of the tank wall under each seismic ground motion are shown from Fig. 18–27. It can be seen that the distributions of the effective stresses along the wall tank under different seismic ground motions have the same law. From the non-stress point at the tank top, the stress gradually increases downward along the tank wall, reaches the maximum at a height of about 4.4 m from the tank's bottom, and decreases rapidly from the maximum location to the bottom of the tank. Under OBE condition, the average ratio of maximum effective stress of LRB isolated tank is reduced to 75.74% of fixed base tank, and that of SVMD isolated tank is reduced to 74.95% of fixed base tank. Under SSE condition, the average ratio of maximum effective stress of LRB isolated tank is reduced to 57.78% of fixed base tank, and that of SVMD isolated tank is reduced to 55.12% of fixed base tank.

Under OBE condition, the maximum effective stresses of SVMD isolated tank are 99.52%, 99.05%, 97.66%, 99.53% and 99.02% of LRB isolated tank, respectively, with the average value reduced to 98.95% of LRB isolated tank. Under SSE condition, the maximum effective stresses of SVMD isolated tank are 96.25%, 94.09%, 94.76%, 92.65% and 99.55% of LRB isolated tank, respectively, with the average value reduced to 95.38% of LRB isolated tank. The maximum effective stresses in the tank walls of both LRB isolated tank and SVMD isolated tank are reduced compared to fixed base tank, and the difference between the maximum effective stresses in the tank walls of LRB isolated tank and SVMD isolated tank is not significant. It can be seen that the SVMD can significantly control the effective stresses on the tank wall. And the higher the peak acceleration of the ground motion, the more obvious the reduction effect of the effective stresses on the tank wall.

4.6. Maximum hydrodynamic pressure

The results of the hydrodynamic pressure analysis of the storage tank are shown in Table 12, the distributions of hydrodynamic pressure along the height of tank wall under each seismic ground motion are shown from Fig. 28–37. It can be seen that the hydrodynamic pressure of fixed base tank is minimum at the liquid surface, gradually increases with decreasing height to a maximum value at a height of 5–10 m. But the hydrodynamic pressure of the isolation tank varies little with the height of the tank wall. Under OBE condition, the average ratio of maximum hydrodynamic pressure of LRB isolated tank is reduced to 20.93% of

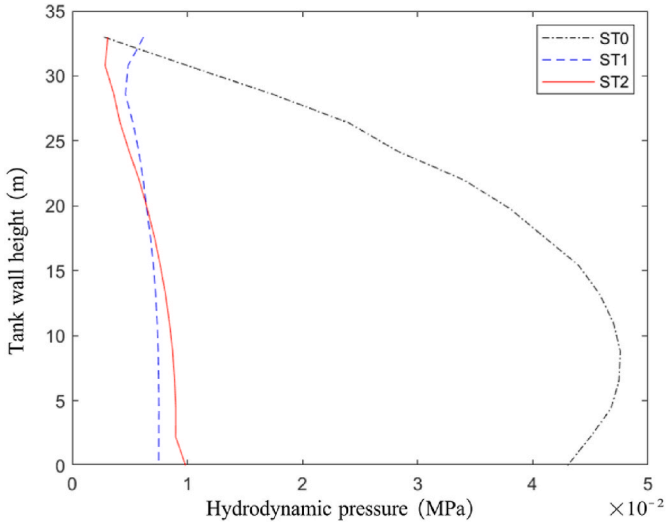

Fig. 28. Distribution of the hydrodynamic pressure (OBE) under the Loma Prieta wave.

Table 12
Comparison of maximum hydrodynamic pressure.

Work Conditions	Structure Type	Maximum Hydrodynamic Pressure (MPa)					
		Loma Prieta	Tottori	Niigata	Chuetsu-oki	Iwate	Average Value
OBE	ST0	0.0476	0.0517	0.0398	0.0543	0.0647	0.0516
	ST1	0.0091	0.0112	0.0133	0.0130	0.0075	0.0108
	ST2	0.0090	0.0101	0.0105	0.0123	0.0068	0.0098
SSE	ST0	0.1410	0.1090	0.1060	0.1560	0.1620	0.1348
	ST1	0.0288	0.0274	0.0335	0.0315	0.0178	0.0278
	ST2	0.0224	0.0185	0.0259	0.0213	0.0172	0.0211

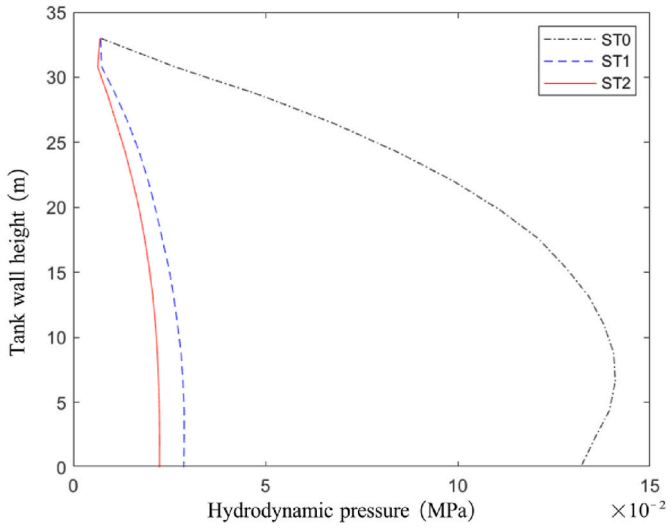

Fig. 29. Distribution of the hydrodynamic pressure (SSE) under the Loma Prieta wave.

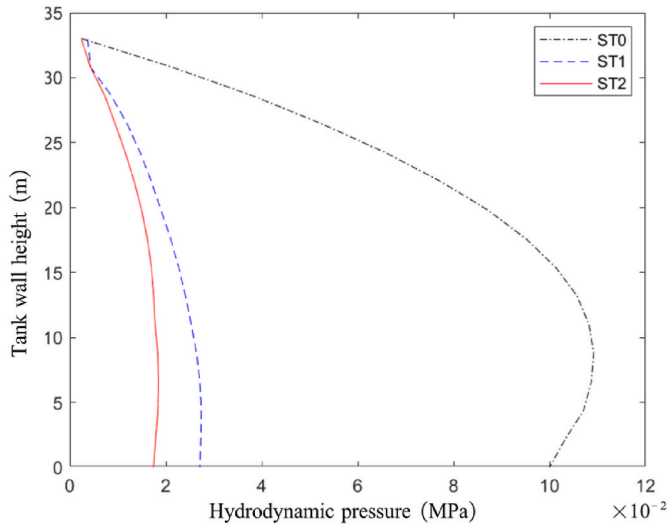

Fig. 31. Distribution of the hydrodynamic pressure (SSE) under the Tottori wave.

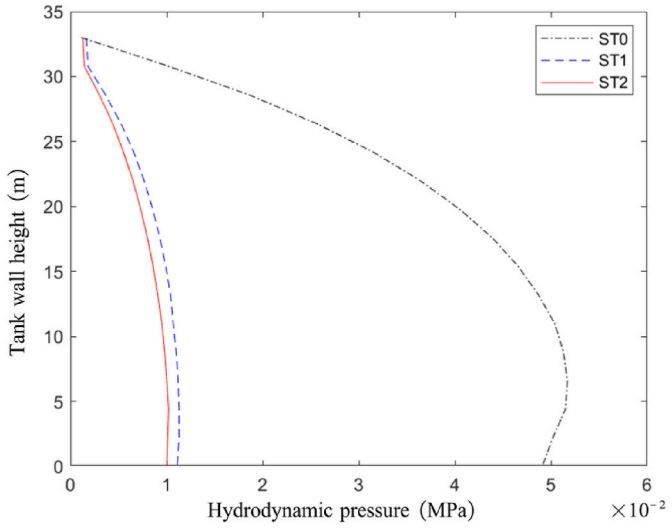

Fig. 30. Distribution of the hydrodynamic pressure (OBE) under the Tottori wave.

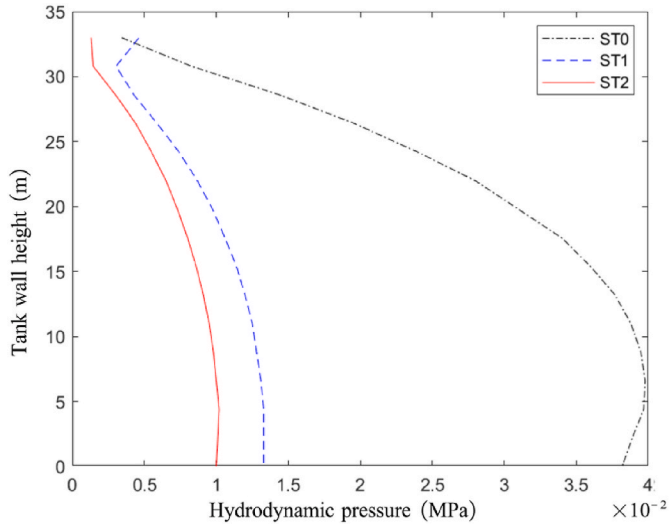

Fig. 32. Distribution of the hydrodynamic pressure (OBE) under the Niigata wave.

fixed base tank, and that of SVMD isolated tank is reduced to 18.99% of fixed base tank. Under SSE condition, the average ratio of maximum hydrodynamic pressure of LRB isolated tank is reduced to 20.62% of fixed base tank, and that of SVMD isolated tank is reduced to 15.65% of fixed base tank.

Under OBE condition, the maximum hydrodynamic pressures of SVMD isolated tank are 98.90%, 90.18%, 78.95%, 94.62% and 90.67% of LRB isolated tank, respectively, with the average value reduced to 90.74% of LRB isolated tank. Under SSE condition, the maximum hydrodynamic pressures of SVMD isolated tank are 77.78%, 67.52%, 77.31%, 67.62% and 96.63% of LRB isolated tank, respectively, with the average value reduced to 75.90% of LRB isolated tank. It can be seen that both the LRB isolated tank, and SVMD isolated tank can significantly control the hydrodynamic pressure on the tank, and the control effect of SVMD is slightly better.

4.7. Influence of liquid level heights

In order to study the seismic mitigation effects of the SVMD isolated tank with different liquid level heights, nonlinear time history analysis is performed on the fixed base tank and the SVMD isolated tank with half tank liquid storage, namely the liquid height is 16.5 m, and is compared to full tank liquid storage's results. The sloshing wave heights and seismic mitigation rates of full tank and half tank are compared in Table 13. It can be seen that whether isolated or non-isolated tanks, the height of the sloshing wave decreases with the decrease of the liquid storage height. The average sloshing wave height of SVMD isolated full tank is reduced by 11.94% and 9.53% compared with that of the fixed base full tank under the OBE and SSE conditions, respectively. The average sloshing wave height of SVMD isolated half tank is reduced by 13.98% and 10.34% compared with that of the fixed base half tank under the OBE and SSE conditions, respectively. The average seismic mitigation rates of the SVMD isolated tank on the wave height increase with decreasing storage height but the effect is not significant.

The maximum effective stresses on the tank wall and the seismic mitigation rates of full and half tank are compared in Table 14. As can be seen from Table 14 that the maximum effective stresses of both seismically isolated and non-isolated tanks decrease as the storage liquid height decreases. The maximum seismic mitigation rates can be maintained above 20% for both full and half tanks under OBE conditions, and

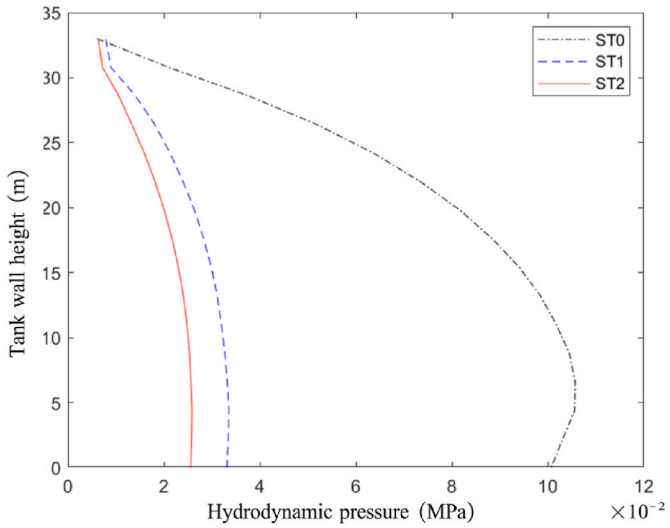

Fig. 33. Distribution of the hydrodynamic pressure (SSE) under the Niigata wave.

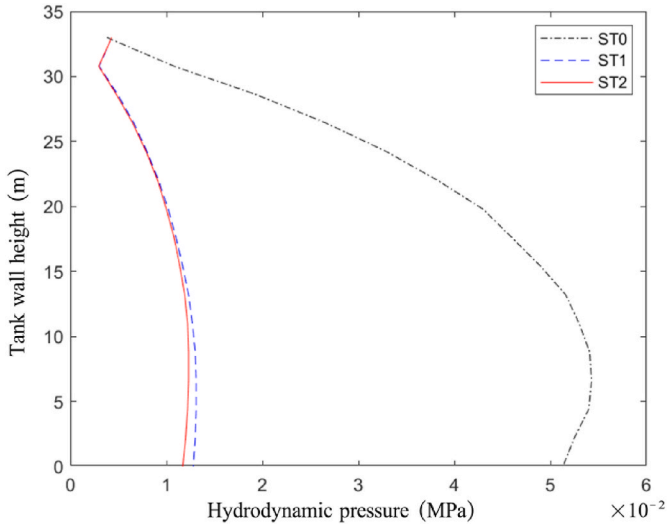

Fig. 34. Distribution of the hydrodynamic pressure (OBE) under the Chuetsu-oki wave.

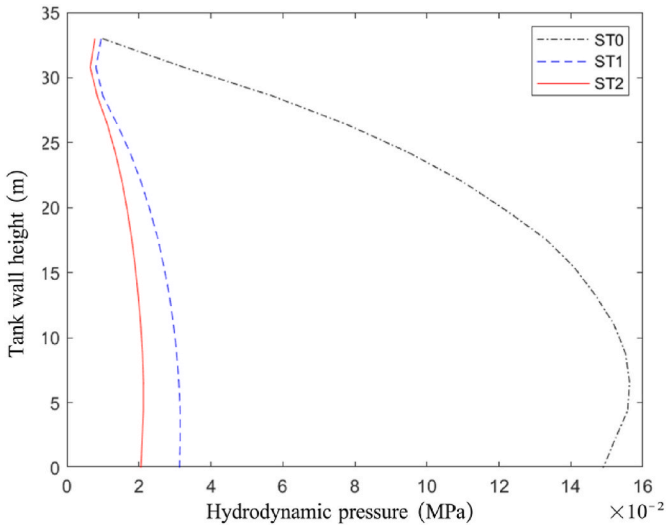

Fig. 35. Distribution of the hydrodynamic pressure (SSE) under the Chuetsu-oki wave.

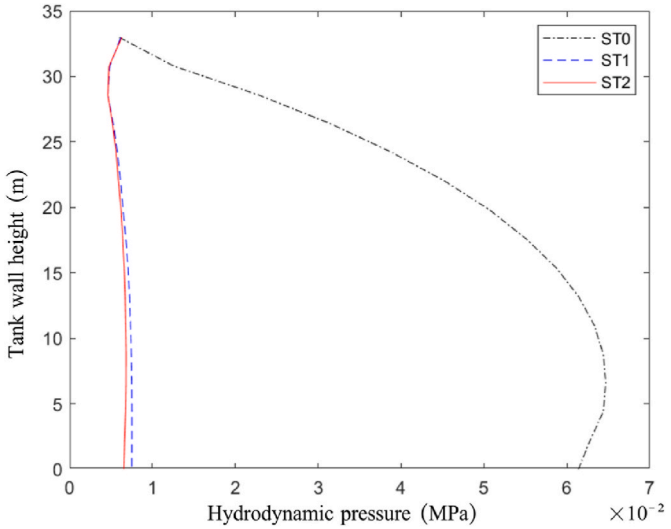

Fig. 36. Distribution of the hydrodynamic pressure (OBE) under the Iwate wave.

above 40% for both full and half tanks under SSE conditions, which proves that the SVMD isolation has good seismic mitigation effects for the effective stress.

The shear-to-weight ratio and seismic mitigation rates of full tank and half tank are compared in Table 15. It can be seen that the average seismic mitigation rates of full tanks are 80.11% and 84.19%, while that of half tanks are 62.36% and 63.33% for OBE and SSE conditions, respectively. It can be concluded that the shear-to-weight ratio mitigation rates of the SVMD isolated tank decrease as the liquid height decreases.

The maximum hydrodynamic pressure and seismic mitigation rates of full tank and half tank are compared in Table 16. It can be seen that the maximum hydrodynamic pressure of both isolated and non-isolated tanks decreases with the decrease of the liquid height. The average seismic mitigation rate of hydrodynamic pressure is more than 80% when the tank is full and more than 70% when the tank is half full.

4.8. *Influence of site conditions*

4.8.1. *Ground motion selection*

In order to study the seismic mitigation effects of SVMD on different site conditions, the ground motion records with characteristic period of 0.45s are selected for nonlinear time history analysis, and are compared to the ground motion records with characteristic period of 0.9s. The site type is Class II according to Chinese seismic design code [19], indicating that the equivalent shear wave velocity of the soil is less than or equal to 500 m/s and greater than 250 m/s, and the site soil cover depth is greater than 5 m. Five natural ground motions are selected as shown in Table 17, and the relationship between ground motions and the Chinese code's response spectrum [19] is shown in Fig. 38.

4.8.2. *Maximum sloshing wave height*

The sloshing wave heights of the SVMD isolated tank under Class II and Class IV site conditions are compared in Table 18. The average values of the sloshing wave heights on Class II site conditions are smaller than those on Class IV site conditions. Under OBE and SSE conditions, the average seismic mitigation rate of the maximum base shear-to-

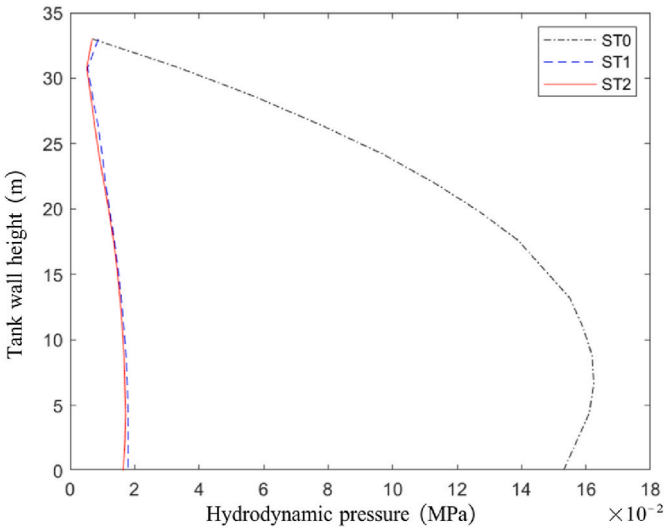

Fig. 37. Distribution of the hydrodynamic pressure (SSE) under the Iwate wave.

weight ratio is reduced by 0.33% and 1.21% for Class II sites compared to Class IV sites, respectively. Therefore, the sloshing wave height is higher and the seismic mitigation effect is lesser the softer the site.

4.8.3. Maximum base displacement

The base displacements of the SVMD isolated tank on Class II and Class IV site conditions are compared in Table 19. The average value of maximum base displacement is 0.023 m on Class II site condition, 0.047 m on Class IV site condition at OBE seismic intensity level. The average value of maximum base displacement is 0.051 m on Class II site condition and 0.1 m on Class IV site condition at SSE seismic intensity level. It can be found that the base displacement of the SVMD isolated tank is more significant in Class IV site.

4.8.4. Maximum base shear

The maximum base shear-to-weight ratios of the SVMD isolated tank on Class II and Class IV site conditions are compared in Table 20. The average value of maximum base shear-to-weight ratio is 0.019 on Class II site condition, 0.045 on Class IV site condition at OBE seismic intensity level. The average value of maximum base shear-to-weight ratio is 0.044 on Class II site condition and 0.091 on Class IV site condition at SSE seismic intensity level. It is found that the base shear of the SVMD isolated tank is greater in Class IV sites, and the seismic mitigation efficiency is poorer. The average seismic mitigation rate of maximum base shear-to-weight ratio is 91.14% on Class II site condition and 80.11% on

Table 13
Sloshing wave heights of full tank and half tank.

Liquid storage height	Seismic wave	Sloshing Wave Height (m)					
		OBE			SSE		
		The fixed base tank	SVMD isolated tank	Seismic mitigation rates	The fixed base tank	SVMD isolated tank	Seismic mitigation rates
Full tank	Loma Prieta	0.677	0.613	9.45%	1.592	1.465	7.98%
	Tottori	0.293	0.259	11.60%	0.55	0.504	8.36%
	Niigata	0.946	0.803	15.12%	1.513	1.340	11.43%
	Chuetsu-oki	0.833	0.652	21.73%	2.357	2.079	11.79%
	Iwate	1.320	1.256	4.85%	1.607	1.505	6.35%
	Average value	0.814	0.717	11.94%	1.524	1.379	9.53%
Half tank	Loma Prieta	0.371	0.333	10.24%	0.841	0.766	8.92%
	Tottori	0.194	0.171	11.86%	0.434	0.391	9.91%
	Niigata	0.744	0.615	17.34%	1.487	1.308	12.04%
	Chuetsu-oki	0.529	0.457	13.61%	1.924	1.693	12.01%
	Iwate	0.751	0.651	13.32%	1.502	1.390	7.46%
	Average value	0.518	0.445	13.98%	1.238	1.110	10.34%

Table 14
Maximum effective stress on the wall of full tank and half tank.

Liquid storage height	Seismic wave	Maximum effective stress (MPa)					
		OBE			SSE		
		The fixed base tank	SVMD isolated tank	Seismic mitigation rates	The fixed base tank	SVMD isolated tank	Seismic mitigation rates
Full tank	Loma Prieta	270	206	23.70%	421	231	45.13%
	Tottori	277	208	24.91%	369	223	39.57%
	Niigata	258	209	18.99%	366	235	35.79%
	Chuetsu-oki	281	212	24.56%	449	227	49.44%
	Iwate	299	203	32.11%	456	220	51.75%
	Average value	277	207.6	25.05%	412.2	227.2	44.88%
Half tank	Loma Prieta	112	87	22.32%	159	99	37.74%
	Tottori	116	89	23.28%	169	105	37.87%
	Niigata	143	111	22.38%	229	110	51.97%
	Chuetsu-oki	117	90	23.08%	171	105	38.60%
	Iwate	142	106	25.35%	226	119	47.35%
	Average value	126	96.6	23.33%	190.8	107.6	43.61%

Table 15
Shear-to-weight ratio of full tank and half tank.

Liquid storage height	Seismic wave	Maximum Base Shear/Weight					
		OBE			SSE		
		The fixed base tank	SVMD isolated tank	Seismic mitigation rates	The fixed base tank	SVMD isolated tank	Seismic mitigation rates
Full tank	Loma Prieta	0.252	0.048	80.95%	0.571	0.109	80.91%
	Tottori	0.212	0.037	82.55%	0.543	0.093	82.87%
	Niigata	0.164	0.045	72.56%	0.446	0.099	77.80%
	Chuetsu-oki	0.228	0.043	81.14%	0.642	0.092	85.67%
	Iwate	0.265	0.05	81.13%	0.683	0.063	90.78%
	Average value	0.224	0.045	80.11%	0.577	0.091	84.19%
Half tank	Loma Prieta	0.085	0.047	44.71%	0.193	0.106	45.08%
	Tottori	0.113	0.055	51.33%	0.256	0.116	54.69%
	Niigata	0.149	0.043	71.14%	0.348	0.104	70.11%
	Chuetsu-oki	0.110	0.054	50.91%	0.249	0.114	54.22%
	Iwate	0.170	0.037	78.24%	0.383	0.084	78.07%
	Average value	0.125	0.047	62.36%	0.286	0.105	63.33%

Table 16
Maximum hydrodynamic pressure of full tank and half tank.

Liquid storage height	Seismic wave	Maximum hydrodynamic pressure (KPa)					
		OBE			SSE		
		The fixed base tank	SVMD isolated tank	Seismic mitigation rates	The fixed base tank	SVMD isolated tank	Seismic mitigation rates
Full tank	Loma Prieta	47.6	9	81.09%	141	22.4	84.11%
	Tottori	51.7	10.1	80.46%	109	18.5	83.03%
	Niigata	39.8	10.5	73.62%	106	25.9	75.57%
	Chuetsu-oki	54.3	12.3	77.35%	156	21.3	86.35%
	Iwate	64.7	6.8	89.49%	162	17.2	89.38%
	Average value	51.62	9.75	81.13%	134.8	21.06	84.38%
Half tank	Loma Prieta	26.9	8	70.26%	60.9	17	72.09%
	Tottori	29.8	9.9	66.78%	67.5	21.4	68.30%
	Niigata	49.3	11.7	76.27%	111.6	25.4	77.24%
	Chuetsu-oki	30.5	10.2	66.56%	69.2	21.1	69.51%
	Iwate	48.1	7	85.45%	109.1	15.7	85.61%
	Average value	36.92	9.36	74.65%	83.66	20.12	75.95%

Table 17
Basic information of ground motion records with characteristic period of 0.45s.

Year	Ground motion records	Magnitude of earthquake	Distance from the epicenter	Shear wave velocity
1971	San Fernando	6.66	39.45	298.68
1978	Tabas Iran	7.35	24.07	324.57
1979	Imperial Valley	6.53	12.69	348.69
1992	Landers	7.28	62.98	367.43
1999	Chi-Chi Taiwan	6.2	24.58	438.19

Class IV site condition at OBE seismic intensity level. The average seismic mitigation rate of maximum base shear-to-weight ratio is 90.58% on Class II site condition and 84.19% on Class IV site condition at SSE seismic intensity level. The results showed that the average seismic mitigation rate of maximum base shear-to-weight ratio is reduced by 11.03% and 6.39% for Class II sites compared to Class IV sites under OBE and SSE conditions, respectively.

4.8.5. Maximum effective stress

The maximum effective stresses on the tank wall of the SVMD isolated tank on Class II and Class IV site conditions are compared in Table 21. The maximum effective stresses on the tank wall of the fixed base tank and the SVMD isolated tank are not significantly affected by the site conditions. Under OBE and SSE conditions, the average seismic mitigation rate of maximum effective stress is reduced by 3.82% and 1.47% for Class II sites compared to Class IV sites, respectively. There is a slight decrease in seismic isolation effect under Class IV site compared with Class II site.

4.8.6. Maximum hydrodynamic pressure

The peak hydrodynamic pressure of the SVMD isolated tank on Class II and Class IV site conditions are compared in Table 22. It can be found that the average value of the peak hydrodynamic pressure of the SVMD isolated tank increases significantly with the decrease of the shear wave velocity of the site soil. Under OBE and SSE conditions, the average seismic mitigation rate of maximum hydrodynamic pressure is reduced by 8.83% and 5.53% for Class II sites compared to Class IV sites, respectively.

4.9. Influence of SVMD parameters

To study the influence of SVMD parameters on the seismic mitigation effects, nine finite element models of SVMD isolated tanks with different additional equivalent damping C_d and additional equivalent mass m_r are subjected to nonlinear time history analysis. The additional equivalent damping C_d is set as $0.6C_i$, $0.8C_i$, C_i, and the additional equivalent mass m_r is set as $0.4m_i$, $0.6m_i$, $0.8m_i$, respectively. The Chuetsu-oki seismic ground motion on Class IV site condition is used to perform the nonlinear time history analysis. Seismic responses of the SVMD isolated

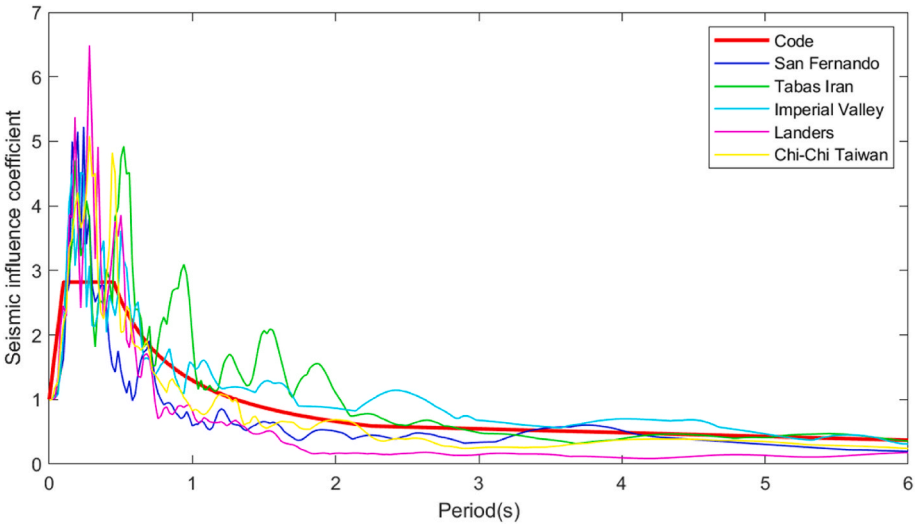

Fig. 38. Acceleration response spectrum.

Table 18
Sloshing wave heights on Class II and Class IV sites.

Site Type	Seismic wave	Sloshing Wave Height (m)					
		OBE			SSE		
		The fixed base tank	SVMD isolated tank	Seismic mitigation rates	The fixed base tank	SVMD isolated tank	Seismic mitigation rates
Class II	San Fernando	0.441	0.384	12.93%	1.049	0.941	10.30%
	Tabas Iran	0.394	0.343	12.94%	0.950	0.879	7.47%
	Imperial Valley	1.334	1.202	9.90%	3.074	2.793	9.14%
	Landers	0.245	0.194	20.82%	0.655	0.489	25.34%
	Chi-Chi Taiwan	0.463	0.401	13.39%	1.077	0.972	9.75%
	Average value	0.575	0.505	12.27%	1.361	1.215	10.74%
Class IV	Loma Prieta	0.677	0.613	9.45%	1.592	1.465	7.98%
	Tottori	0.293	0.259	11.60%	0.550	0.504	8.36%
	Niigata	0.946	0.803	15.12%	1.513	1.340	11.43%
	Chuetsu-oki	0.833	0.652	21.73%	2.357	2.079	11.79%
	Iwate	1.320	1.256	4.85%	1.607	1.505	6.35%
	Average value	0.814	0.717	11.94%	1.524	1.379	9.53%

Table 19
Maximum base displacement on Class II and Class IV sites.

Site Type	Seismic wave	Maximum Base Displacement (m)			
		OBE		SSE	
		The fixed base tank	SVMD isolated tank	The fixed base tank	SVMD isolated tank
Class II	Loma Prieta	0	0.056	0	0.120
	Tottori	0	0.040	0	0.085
	Niigata	0	0.049	0	0.108
	Chuetsu-oki	0	0.047	0	0.104
	Iwate	0	0.052	0	0.081
	Average value	0	0.049	0	0.100
Class IV	San Fernando	0	0.022	0	0.048
	Tabas Iran	0	0.032	0	0.071
	Imperial Valley	0	0.026	0	0.057
	Landers	0	0.014	0	0.030
	Chi-Chi Taiwan	0	0.021	0	0.048
	Average value	0	0.023	0	0.051

tanks with different parameters are compared in Table 23.

The results of Table 23 show that the sloshing wave height and the shear-to-weight ratio decrease with the increase of additional equivalent mass, while the base displacement remains the same. The sloshing wave height, base shear and base displacement of the tank decrease with the increase of the additional equivalent damping. Therefore, increasing the additional equivalent damping of the SVMD can reduce the seismic responses of the structure, and increasing the additional equivalent mass can reduce the sloshing wave height, but cannot reduce the base shear. Thus, the equivalent additional damping can take a large value, but the equivalent additional mass should be controlled within a suitable range to avoid generating excessive base shear.

5. Conclusion

This paper presents the theory and design of a hybrid seismic control system for LNG storage tanks, which combines seismic isolation using series viscous mass damper (SVMD) devices in parallel with LRB isolators. A specific LNG storage tank engineering example is designed to demonstrate the effectiveness of hybrid seismic isolation. Nonlinear time history analysis is conducted to analyze and compare the seismic mitigation effects of a fixed base tank, an LRB isolated tank, and an SVMD isolated tank. Additionally, the effects of different site conditions, varying storage liquid levels, and changes in SVMD parameters on the seismic isolation performance are investigated. The following conclusions are drawn based on the results obtained from simulation analysis.

Table 20
Maximum shear-to-weight ratios on Class II and Class IV sites.

Site Type	Seismic wave	Maximum Base Shear/Weight					
		OBE			SSE		
		The fixed base tank	SVMD isolated tank	Seismic mitigation rates	The fixed base tank	SVMD isolated tank	Seismic mitigation rates
Class II	San Fernando	0.209	0.018	91.32%	0.343	0.041	88.08%
	Tabas Iran	0.273	0.027	90.08%	0.619	0.061	90.08%
	Imperial Valley	0.156	0.022	86.05%	0.353	0.049	86.05%
	Landers	0.211	0.011	94.68%	0.478	0.025	94.71%
	Chi-Chi Taiwan	0.230	0.018	92.38%	0.521	0.041	92.13%
	Average value	0.216	0.019	91.14%	0.463	0.044	90.58%
Class IV	Loma Prieta	0.252	0.048	80.95%	0.571	0.109	80.91%
	Tottori	0.212	0.037	82.55%	0.543	0.093	82.87%
	Niigata	0.164	0.045	72.56%	0.446	0.099	77.80%
	Chuetsu-oki	0.228	0.043	81.14%	0.642	0.092	85.67%
	Iwate	0.265	0.05	81.13%	0.683	0.063	90.78%
	Average value	0.224	0.045	80.11%	0.577	0.091	84.19%

Table 21
Maximum effective stress on the tank wall on Class II and Class IV sites.

Site Type	Seismic wave	Maximum Effective Stress (MPa)					
		OBE			SSE		
		The fixed base tank	SVMD isolated tank	Seismic mitigation rates	The fixed base tank	SVMD isolated tank	Seismic mitigation rates
Class II	San Fernando	278	200	28.06%	388	211	45.62%
	Tabas Iran	315	206	34.60%	474	225	52.53%
	Imperial Valley	260	203	21.92%	347	217	37.46%
	Landers	277	202	27.08%	387	216	44.19%
	Chi-Chi Taiwan	290	199	31.38%	415	210	49.40%
	Average value	284	202	28.87%	402	216	46.35%
Class IV	Loma Prieta	270	206	23.70%	421	231	45.13%
	Tottori	277	208	24.91%	369	223	39.57%
	Niigata	258	209	18.99%	366	235	35.79%
	Chuetsu-oki	281	212	24.56%	449	227	49.44%
	Iwate	299	203	32.11%	456	220	51.75%
	Average value	277	208	25.05%	412	227	44.88%

Table 22
Maximum hydrodynamic pressure of Class II and Class IV sites.

Site Type	Seismic wave name	Maximum Hydrodynamic Pressure (KPa)					
		OBE			SSE		
		The fixed base tank	SVMD isolated tank	Seismic mitigation rates	The fixed base tank	SVMD isolated tank	Seismic mitigation rates
Class II	San Fernando	51.7	5.19	89.96%	117	11.8	89.91%
	Tabas Iran	73.3	8.77	88.04%	167	19.9	88.08%
	Imperial Valley	40.4	6.78	83.22%	91.9	15.4	83.24%
	Landers	51.0	6.74	86.78%	116	15.3	86.81%
	Chi-Chi Taiwan	57.9	5.01	91.35%	132	10.9	91.74%
	Average value	51.7	5.19	89.96%	117	11.8	89.91%
Class IV	Loma Prieta	47.6	9	81.09%	141	22.4	84.11%
	Tottori	51.7	10.1	80.46%	109	18.5	83.03%
	Niigata	39.8	10.5	73.62%	106	25.9	75.57%
	Chuetsu-oki	54.3	12.3	77.35%	156	21.3	86.35%
	Iwate	64.7	6.8	89.49%	162	17.2	89.38%
	Average value	51.62	9.75	81.13%	134.8	21.06	84.38%

The base shear, effective stress, and hydrodynamic pressure of the LRB isolated tanks were reduced to 20.64%, 75.74%, and 20.93% of the fixed base tank at OBE and 17.41%, 57.78%, and 20.62% of the fixed base tank at SSE, respectively. The sloshing wave heights of LRB isolated tank are 8.53% and 16.82% larger than those of the fixed base tank under OBE and SSE conditions.

Although the ordinary LRB seismic isolation bearing can effectively reduce the effective stress the tank wall, hydrodynamic pressure and base shear, it has an amplifying effect on the sloshing wave height of the storage fluid. The seismically isolated tank with SVMD not only has the seismic mitigation effect of ordinary LRB, but also has a good control effect on the sloshing wave height of the storage fluid.

The sloshing wave height, base shear, effective stress, and hydrodynamic pressure of the SVMD isolated tanks were reduced to 88.06%, 19.81%, 74.95% and 18.99% of the fixed base tank at OBE and 90.47%, 15.78%, 55.12% and 15.65% of the fixed base tank at SSE, respectively. The increase of seismic response will reduce the effect of SVMD on wave height control.

Under the OBE seismic intensity level, the seismic mitigation rates of the SVMD isolated half tank for maximum effective stress, base shear and hydrodynamic pressure is 1.72%, 17.75% and 6.48% lower than that of full tank. Under the SSE seismic intensity level, they are 1.21%,

Table 23
Seismic responses of the SVMD isolated tanks with different parameters.

m_r	Maximum Response	C_d			
		$0.6C_i$	$0.8C_i$	C_i	Average
$0.4m_i$	Base displacement (m)	0.10	0.10	0.10	0.10
	Shear-to-weight ratio	0.085	0.083	0.082	0.083
	Sloshing wave height (m)	2.19	2.13	2.08	2.13
$0.6m_i$	Base displacement (m)	0.11	0.10	0.10	0.10
	Shear-to-weight ratio	0.096	0.092	0.090	0.093
	Sloshing wave height (m)	2.13	2.08	2.02	2.08
$0.8m_i$	Base displacement (m)	0.11	0.10	0.10	0.10
	Shear-to-weight ratio	0.102	0.100	0.098	0.100
	Sloshing wave height (m)	2.07	2.02	1.97	2.02

20.86% and 8.43% lower than that of full tank. It can be seen that the seismic reduction effect of SVMD increases with the increase of storage height.

The greater the thickness of the site cover soil and the lower the shear wave velocity, the greater the seismic responses of the SVMD isolated tank and the worse the seismic isolation effects. Under the SSE seismic intensity level, the seismic mitigation rates of the SVMD isolated tank for sloshing wave height, base shear and maximum hydrodynamic pressure on Class IV site are 1.21%, 6.39% and 5.53% lower than that in Class II site.

The increase of SVMD's additional equivalent mass reduces the sloshing wave height, increases the shear-to-weight ratio, and has little influence on the base displacement. The increase of SVMD's additional equivalent damping reduce the sloshing wave height, base shear force and base displacement of the tank. Therefore, in order to ensure the seismic mitigation effect of SVMD isolated tank, the additional equivalent damping can take a large value, but the additional equivalent mass should be controlled within a suitable range to avoid excessive base displacement.

CRediT author statement

Chao Luo: Investigation, Validation, Writing - Original Draft, Writing - Review & Editing, Funding acquisition, Hao-Ran Mu: Formal analysis, Hao Wang: Formal analysis, Visualization, Funding acquisition, Xiao-Xia Guo: Writing - Review & Editing, Dong-Lin Liu: Conceptualization, Data processing, Huai-Ping Feng: Resources, Supervision, Funding acquisition.

Declaration of competing interest

The authors declare that they have no known competing financial interests or personal relationships that could have appeared to influence the work reported in this paper.

Data availability

Data will be made available on request.

Acknowledgments

This study was funded by the independent projects for State Key Laboratory of Mechanical Behavior and System Safety of Traffic Engineering Structures [grant numbers ZZ2020-04, ZZ2021-03]; the project for the introduction of overseas students in Hebei Province (CN) [grant number C20190364]; the Natural Science Foundation of Hebei Province (CN) [grant number E202210095]; S&T Program of Hebei (CN) [grant number 21375407D].

References

[1] Chalhoub MS, Kelly JM. Shake table test of cylindrical water tanks in base-isolated structures[J]. J Eng Mech 1990;116(7):1451–72.
[2] Malhotra PK. Method for seismic base isolation of liquid-storage tanks[J]. J Struct Eng 1997;123(1):113–6.
[3] Shrimali MK, Jangid RS. Non-linear seismic response of base-isolated liquid storage tanks to bi-directional excitation[J]. Nucl Eng Des 2002;217(1):1–20.
[4] Curadelli O. Equivalent linear stochastic seismic analysis of cylindrical base-isolated liquid storage tanks[J]. J Constr Steel Res 2013;83:166–76.
[5] Christovasilis IP, Whittaker AS. Seismic analysis of conventional and isolated LNG tanks using mechanical analogs[J]. Earthq Spectra 2008;24(3):599–616.
[6] Wang Y, Teng M, Chung K. Seismic isolation of rigid cylindrical tanks using friction pendulum bearings[J]. Earthq Eng Struct Dynam 2001;30(7):1083–99.
[7] Shrimali MK, Jangid RS. A comparative study of performance of various isolation systems for liquid storage tanks[J]. Int J Struct Stabil Dynam 2011;2(4):573–91.
[8] Yu Q, Wu J, Gu X, et al. Experimental study on effects of U-shape dampers on earthquake responses of a base-isolated LNG inner tank[J]. Eng Struct 2022;269:114841.
[9] Cheng X, Jing W, Gong L. Simplified model and energy dissipation characteristics of a rectangular liquid-storage structure controlled with sliding base isolation and displacement-limiting devices[J]. J Perform Constr Facil 2017;31(5).
[10] Zhang L, Guo M, Li Z, et al. Optimal design and seismic performance of base-isolated storage tanks using friction pendulum inerter systems. J. Struct. 2022;43:234–48.
[11] Rawat A, Matsagar V. Seismic analysis of liquid storage tank using oblate spheroid base isolation system based on rolling friction[J]. Int J Non Lin Mech 2022:104186.
[12] Malhotra PK. Seismic strengthening of liquid-storage tanks with energy-dissipating anchors[J]. J Struct Eng 1998;124(4):405–14.
[13] De Angelis M, Giannini R, Paolacci F. Experimental investigation on the seismic response of a steel liquid storage tank equipped with floating roof by shaking table tests[J]. Earthq Eng Struct Dynam 2010;39(4):377–96.
[14] Kharde SH, Soni DP. Seismic response mitigation of extra-large LNG storage tanks [J]. J. Earthq. Tsunami 2022;16(5).
[15] Hao L, Zhang R, Weng D. A hybrid control method to reduce the seismic response of a liquid storage tank: Asme pressure vessels & piping conference. 2016 [C].
[16] Zhang R, Zhao Z, Pan C. Influence of mechanical layout of inerter systems on seismic mitigation of storage tanks[J]. Soil Dynam Earthq Eng 2018;114:639–49.
[17] Jiang Y, Zhao Z, Zhang R, et al. Optimal design based on analytical solution for storage tank with inerter isolation system[J]. Soil Dynam Earthq Eng 2020;129:105924.
[18] GB 50341-2014 Code for design of vertical cylindrical welded steel oil tanks[S]. Beijing: Standards Press of China; 2014.
[19] GB 50011-2010 Code for seismic design of buildings[S]. Beijing: Standards Press of China.